Low-Lying Electronic States, Spectroscopy, and Photophysics of Linear Para Acenequinones

Takao Itoh

Science Laboratory, Kanto Junior College, 625 Oya-cho, Tatebayashi, Gunma 374, Japan

Received November 22, 1994 (Revised Manuscript Received September 5, 1995)

Contents

Takao Itoh was born in Tokyo, Japan, in 1951. He graduated from Hokkaido University where he received a B.Sc. degree in chemistry under the direction of Professor Kimio Ohno in 1974, and M.Sc. and D.Sc. degrees under the direction of Professor Hiroaki Baba, in 1976 and 1979, respectively. From 1980 to 1992 he worked for research divisions of chemical companies, except for 1985–1986 during which he was a Research Associate collaborating with Professor Bryan Kohler at the University of California, Riverside. Since 1993, he has been an Associate Professor of Science at Kanto Junior College. He is the author or co-author of over 60 scientific papers on physical chemistry, solid-state physics, and material science and 30 Japanese patents. In addition to his interests in physical chemistry, Takao Itoh is an entomologist and a member of the Lepidopterists' Society (United States), as well as the Chemical Society of Japan, and American Chemical Society. He has written also 15 papers on Lepidoptera.

I. Introduction

Para quinones play an important role in biological systems such as vitamin K_1 or K_3 and in functional materials such as organic photoconductors as well as in dyestuffs.[1-3] A detailed understanding of para quinone electronic states is not merely the foundation on which an understanding at the molecular level of such an important role must rest, but the starting point to reveal the relationship between the electronic structure and dynamical behavior as well. Although the spectroscopy of para quinones has a long history, it still remains an attractive area.[4]

One of the prominent features of the electronic states of para quinones is the existence of two excited (n,π^*) states. Due to the existence of two C=O groups, these molecules possess two nonbonding orbitals, n_+ and n_-, that are nearly localized on the two oxygen atoms. Promotion of an electron from one of the occupied nonbonding orbitals to one of the vacant π^* orbitals generates an excited (n,π^*) state. This means that at least two types of (n,π^*) states, (n_-,π^*) and (n_+,π^*), are always possible. The lowest (n,π^*) state of smaller quinones is located lower in energy than the lowest (π,π^*) states, but as the size of quinones is increased the state ordering inverts.

Some of these molecules are known to exhibit interesting photophysical properties. 1,4-Naphthoquinone, for example, exhibits dual phosphorescence from the $^3(n_-,\pi^*)$ and $^3(n_+,\pi^*)$ states in addition to the $S_1(n,\pi^*)$ fluorescence in the vapor phase as well as in a CCl_4 solution.[5,6] Fluorescence from a singlet–triplet mixed state also has been observed for 1,4-naphthoquinone and *p*-benzoquinone in the vapor phase at low pressure (10^{-2}–10^{-3} Torr)[7-9] and in a supersonic jet expansion for the latter molecule.[10,11] These emission properties are determined by the state ordering and the nature of the excited electronic states.

In order to understand the relationship between the electronic structure and the photophysical properties of these molecules, it is of initial importance to examine the spectroscopic data so far obtained. To date, there are no systematic review articles that describe the electronic spectra, states, and photophysics of a family of linear para acenequinones, despite the fact that there are numerous publications and researchers concerned with this family. It is the goal of this review to highlight some of the more interesting emission properties and photophysics of quinones comprehensively and critically based upon what is known spectroscopically about the excited electronic states and the dynamical behavior. We

0009-2665/95/0795-2351$15.50/0

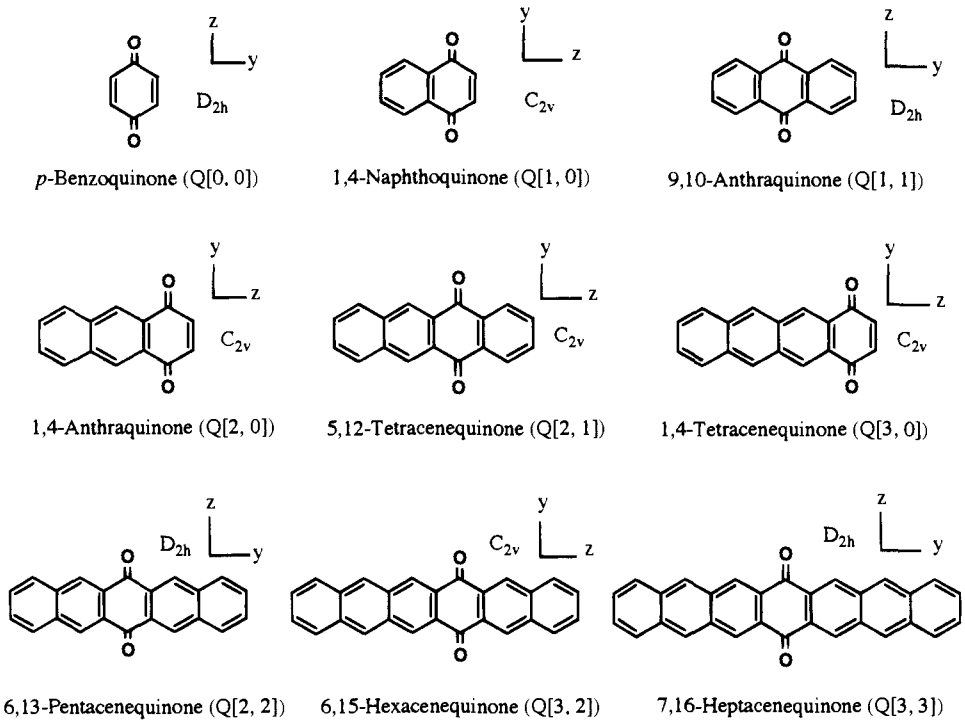

Figure 1. Linear para acenequinones with the coordinate systems treated in the present review.

will concern ourselves mainly with a discussion of the intrinsic properties of the molecules. Thus, the phenomena relating to intermolecular interactions such as hydrogen-bonding effects are not discussed here.

Linear para acenequinones form a unique group of organic molecules for which a number of modern techniques should be applied to get more detailed information on the photophysical properties. It is anticipated that the present review will serve as a resource for scientists working to understand seemingly complicated spectroscopic data, electronic states, photophysics, and photochemistry of para acenequinones as well as for those who are dealing with the photophysics of medium-size molecules other than quinones.

Only nine unsubstituted linear para acenequinones have been investigated spectroscopically up to now. It is beyond the scope of the present review to discuss the electronic states and spectra of all the substituted para quinones so far studied. For the sake of clarity this article will focus mainly on an analysis of the lower lying electronic states of the nine molecules illustrated in Figure 1.

II. Symmetry of the Electronic States

The systems treated in the present article are all highly symmetric molecules that belong to either the C_{2v} or D_{2h} point group. The chemical formula of these molecules can be expressed as $C_{[4(m+n)+6]}O_2H_{[2(m+n)+4]}$ (m, n = 0, 1, 2, 3,...) and the number of the isomeric para quinones is given by $(m + n + 1)/2$ for the systems with odd $(m + n)$, and by $(m + n + 2)/2$ for those with even $(m + n)$. Nepras and Titz introduced the symbol Q[m,n] to specify a particular unsubstituted linear para acenequinone (refer to the scheme shown below):[12] Q[m,n] with $m > n$ and those with $m = n$ stand for the C_{2v} and D_{2h} quinones, respectively. Considering the low double-bond character of the bonds adjoining the C=O groups and the lowering of the conjugation connected with them, this symbol is a convenient presentation also in displaying the electronic-state levels of these systems.[12,13] In the present article all the systems are indicated by this symbol.

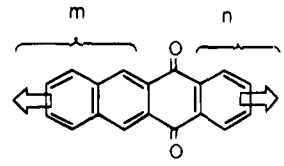

Unfortunately, the coordinate of para quinones has been defined differently by different researchers, and perhaps this has given rise to some confusion in the literature. In this review, **the axis parallel to the two C=O bonds is defined as *y* for C_{2v} quinones and as *z* for D_{2h} quinones, and the *x*-axis is taken to lie perpendicular to the molecular plane** as indicated in Figure 1. Hence, it must be kept in mind that in some case the symmetry presentations used in this article are different from those used in the original papers.

In order to facilitate a discussion of the electronic states and spectroscopy, it is convenient to describe briefly the symmetry of the electronic states in the beginning. The ground states are characterized by A_1 and A_g symmetry, respectively, for the C_{2v} and D_{2h} quinones. In the first approximation, the sum and difference of the two in-plane n orbitals on the oxygen atoms $n_1 + n_2$ and $n_1 - n_2$ give rise to the molecular orbitals n_+ and n_-, respectively. The n_+ and n_-

molecular orbitals of all the C_{2v} quinones are of a_1 and b_2 symmetry, respectively, while the π molecular orbitals are either a_2 or b_1. Hence, the excited (n,π^*) states are either A_2 (= $a_1 \times a_2$ or $b_2 \times b_1$) or B_1 (= $a_1 \times b_1$ or $b_2 \times a_2$), while the (π,π^*) states are either A_1 (= $a_2 \times a_2$ or $b_1 \times b_1$) or B_2 (= $a_2 \times b_1$) for the C_{2v} quinones. The n_+ and n_- molecular orbitals of the D_{2h} quinones are of b_{2u} and b_{3g} symmetry, respectively, while the π molecular orbitals have either b_{1g}, b_{2g}, b_{3u}, or a_u symmetry. Referring to the character table for the D_{2h} point group, one can easily recognize that the excited (n,π^*) states are either B_{1g}, B_{2g}, B_{3u}, or A_u and that the (π,π^*) states are either B_{1u}, B_{2u}, B_{3g}, or A_g. As far as the low-lying (n,π^*) states are concerned, to a first approximation, it is sufficient to consider only the n and π^* orbitals with high AO coefficients on the C=O groups. Since the π^* orbitals on the C=O groups of the D_{2h} quinones are either b_{3u} or b_{2g}, the low lying $^{1,3}(n,\pi^*)$ states are either $^{1,3}A_u$ or $^{1,3}B_{1g}$: Both of the electron promotions $n_+(b_{2u}) \rightarrow \pi^*(b_{2g})$ and $n_-(b_{3g}) \rightarrow \pi^*(b_{3u})$ can produce the A_u state, while both of $n_+ \rightarrow \pi^*(b_{3u})$ and $n_- \rightarrow \pi^*(b_{2g})$ can produce the B_{1g} state. Further, it is easily shown for all the D_{2h} quinones that the $^1A_g \rightarrow {}^3A_u$ transition is expected to be stronger than the $^1A_g \rightarrow {}^3B_{1g}$ transition (Appendix A), for which a more detailed interpretation has been given by Hollas and Goodman for *p*-benzoquinone (Q[0,0]).[14]

III. Spectroscopic Determination of the Excited Electronic States

In order to understand the emission and photophysical properties, it is essential to possess a detailed knowledge on the location and nature of the excited states, together with information on the vibronic and/or spin–orbit interactions between them. Although the determination of the excited states of the present systems has been based mostly upon the measurements of absorption, emission, and excitation spectra, it has a long and complicated history. Nevertheless, the locations of all the low-lying excited states have not been settled yet even for typical para quinones. One of the difficulties in the state assignments arises from the fact that the four low-lying states, $^{1,3}(n_+,\pi^*)$ and $^{1,3}(n_-,\pi^*)$, are nearly degenerate. The other difficulty lies in the separation of major bands from site or phonon bands in Shpolskii spectra, but such spectra have also advantages for identifications of the excited states. In Shpolskii matrices, each level occupies a very narrow energy range, showing extremely sharp spectra. Examples of such spectra are displayed in Figure 2 for Q[1,0] and Q[2,1], together with the spectra in rigid glasses at 77 K.[15] As will be mentioned later in detail, the phosphorescence of Q[1,0] originates from the $^3(n,\pi^*)$ state, while that of Q[2,1] originates from $^3(\pi,\pi^*)$. These two spectra exhibit clearly the difference between the nature of the two excited triplet states: The spectrum of Q[1,0] shows the prominent feature in the C=O stretching vibration, while that of Q[2,1] shows the feature based on the aromatic ring vibrations.

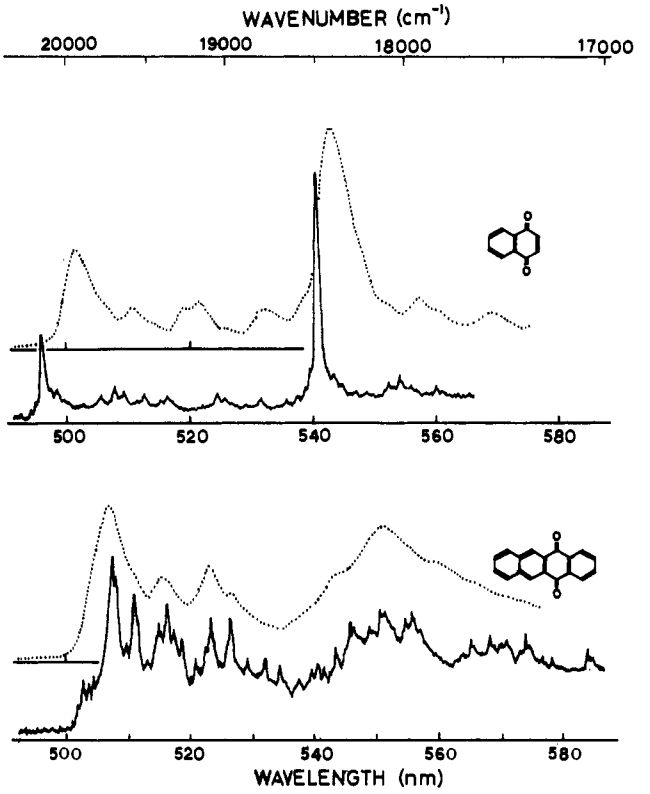

Figure 2. Phosphorescence spectra of Q[1,0] and Q[2,1] in an isopentane–methylcyclohexane mixture at 77 K (dotted line spectra) and in *n*-pentane (Q[1,0]) or in *n*-hexane (Q[2,1]) at 13 K (solid line spectra).[15]

A. *p*-Benzoquinone

p-Benzoquinone (Q[0,0]) is the simplest para quinone for which a vast number of spectroscopic studies have been carried out. The absorption spectra have been obtained in the vapor phase,[16–23,41,42] in solutions,[18,24–32,40] in a rigid glass,[33] and in pure[22,34–39] and mixed crystalline states.[38] The first curve in Figure 3a presents the absorption spectrum of Q[0,0] in hexane. The strong absorption band at about 40 000 cm^{-1} with the molar extinction coefficient $\epsilon \sim 20\,000$ and the shoulder band at ~33 000 cm^{-1} ($\epsilon \sim 1300$) are both due to transitions to the $^1(\pi,\pi^*)$ states. The former band has been assigned as due to $^1A_g \rightarrow {}^1B_{1u}$,[34,35] while the latter band has been attributed to the $^1A_g \rightarrow {}^1B_{3g}$ transition which borrows the intensity through vibronic coupling with the former transition.[22] The weak visible absorption ($\epsilon \sim 20$) ranging from 20 000 to 27 000 cm^{-1} corresponds to the excitation into the $^1(n,\pi^*)$ state with the B_{1g} symmetry,[18] although the possibility for presence of the $^1A_u(n,\pi^*)$ state at this absorption region has been pointed out.[24] A much weaker band at about 18 500 cm^{-1} is due to the transition to the $T_2(n,\pi^*)$ state with the A_u symmetry. This $S_0 \rightarrow T_2(^3A_u)$ band has an unusually large ϵ value (~0.3), but Zeeman effect experiments revealed that it is really based on a S → T transition.[21,36] A precise review of the experimental works up to 1971 on the electronic states and spectra of Q[0,0] has been described by Trommsdorff,[22] but partial reviews are seen also in refs 18 and 38. These articles still remain as resources for those who are interested in spectroscopy of Q[0,0].

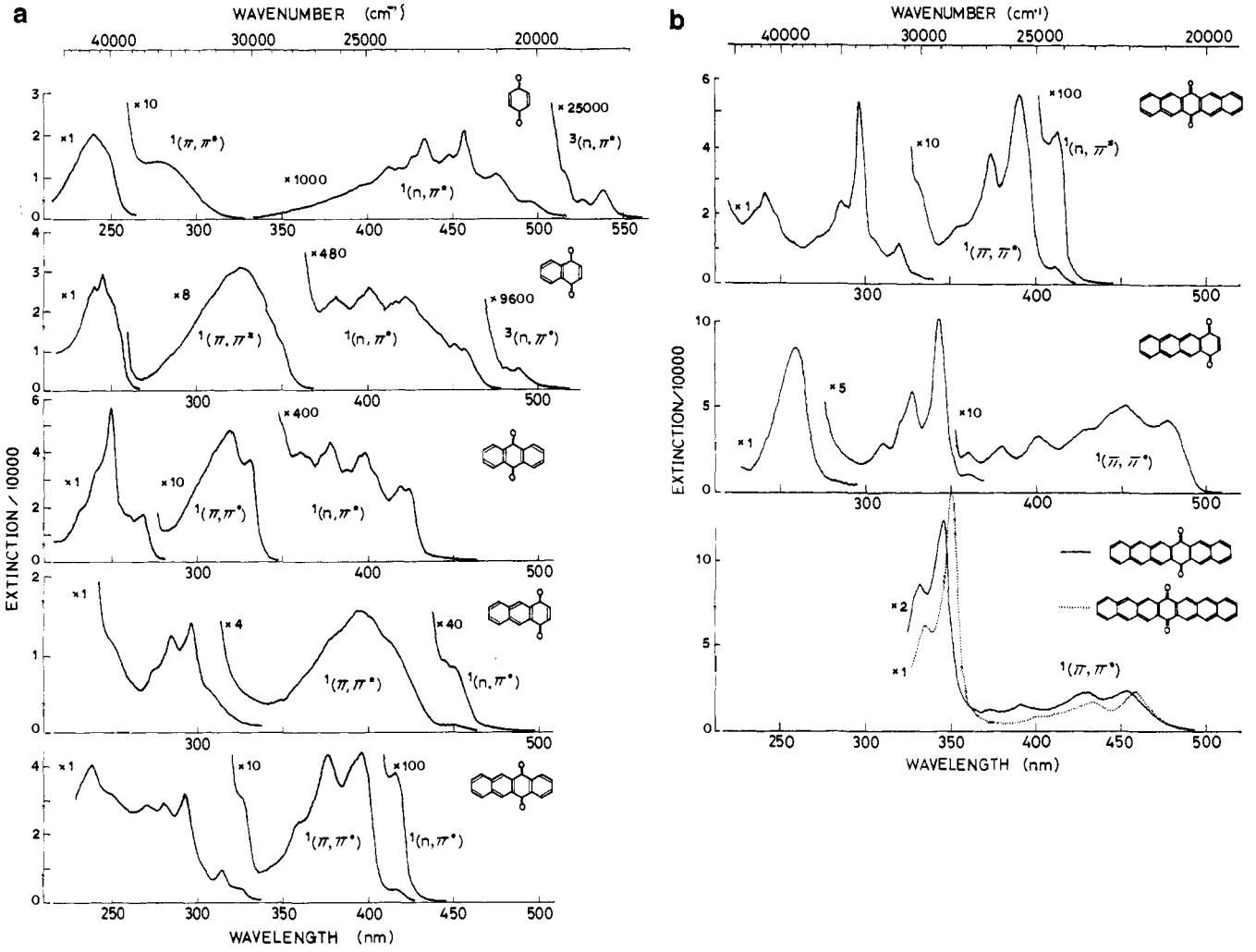

Figure 3. (a) Absorption spectra of Q[0,0], Q[1,0], Q[1,1], Q[2,0], and Q[2,1] in *n*-hexane at room temperature and (b) absorption spectra of Q[2,2] and Q[3,0] in *n*-hexane, and Q[3,2] and Q[3,3] in trichlorobenzene at room temperature. The spectrum of Q[3,0] is taken from ref 135 and those of Q[3,2] and Q[3,3] are taken from ref 72. The spectra for Q[3,0], Q[3,2], and Q[3,3] are converted from the original logarithmic scale spectra.

Most of the experimental and theoretical interests in the electronic spectrum lie in the identification of the four low-lying excited states, $^{1,3}A_u(n,\pi^*)$ and $^{1,3}B_{1g}$ (n,π^*), that are located in a very narrow range, 18300~20100 cm^{-1}. Although the transitions to these four (n,π^*) states have been detected in the absorption spectrum of the pure crystal, the early assignment for the ^1A_u origin was criticized by Dunn and Francis.[39] The origins of the ^1A_u and $^1B_{1g}$ states are basically missing and the transitions to these states are induced mainly through coupling of out-of-plane vibrations with the $^1(\pi,\pi^*)$ states. The $^1A_g \rightarrow {}^3A_u$ absorption band has the vibronic pattern of an allowed transition due to direct spin–orbit coupling, while the $^1A_g \rightarrow {}^3B_{1g}$ transition is induced by vibronic spin–orbit coupling. In static vapor the transitions to only two of these four states ($^1B_{1g}$ and ^3A_u) have been identified in the absorption spectra,[14,18,19] but in a supersonic jet at least three of them (^1A_u, $^1B_{1g}$, and ^3A_u) have been identified in the excitation spectrum.[44,45] The measurements of the emission and excitation spectra have played a crucial role in the determination of the low-lying states.

Emission of Q[0,0] has been observed in mixed crystals,[38,43,46–51] in pure crystal,[52] in a rigid glass,[37,52,57] in a neon host,[58] in a degassed fluid solution,[59] and in the vapor phase.[9,10,11,39,44,45,56–59] The first spectrum in Figure 4 is the emission spectrum of Q[0,0] static vapor. The emission starting from 535.2 nm is the $^3A_u(T_2) \rightarrow {}^1A_g$ phosphorescence which shows a prominent progression in the C=O stretching vibration with a frequency of 1680 cm^{-1} accompanied by the weak combination bands. The weak $^3B_{1g} \rightarrow {}^1A_g$ phosphorescence band also was reported in the vapor phase,[58] but it has not been observed unambiguously in more recent observations.[9,45] The weak emission band on the blue side of the ^3A_u phosphorescence in Figure 4 is the fluorescence from $^1B_{1g}$ which is in thermodynamic equilibrium with ^3A_u.[9] Although some vibrational fine structure of the $^1B_{1g}$ fluorescence has been observed in the static vapor phase,[39] well-resolved fluorescence and phosphorescence spectra as well as their excitation spectra have been obtained in a supersonic jet expansion.[10,11,44,45] In a jet the $^1B_{1g}$ origin was observed at 20 045 cm^{-1}, while the ^1A_u origin was indirectly determined at 19 991 cm^{-1}.[44] (The transitions $^1A_g \rightarrow {}^1B_{1g}$ and $^1A_g \rightarrow {}^1A_u$ are electronic dipole forbidden, but the former is magnetic dipole allowed.) It was indicated that the ^3A_u and $^3B_{1g}$ origins are degenerate within 0.5 cm^{-1} in a jet,[44] but the more detailed information has not been given for this degeneracy.

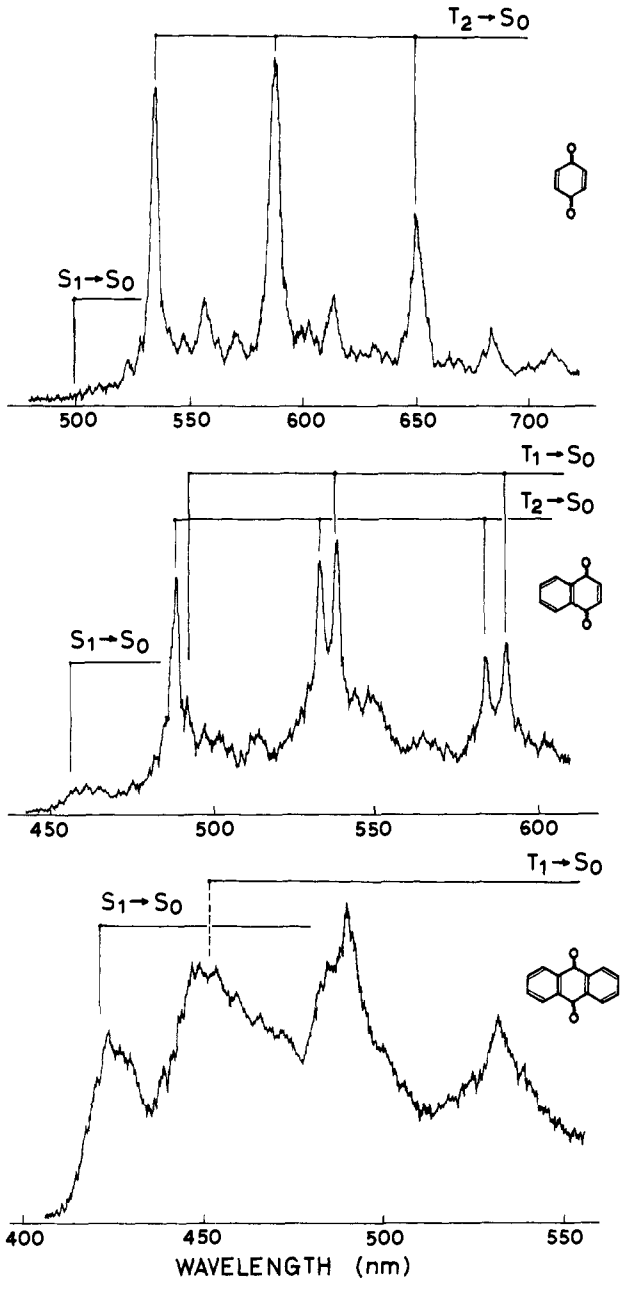

Figure 4. Emission spectra of Q[0,0], Q[1,0], and Q[1,1] static vapors in the presence of an added buffer gas at temperatures near room temperature.

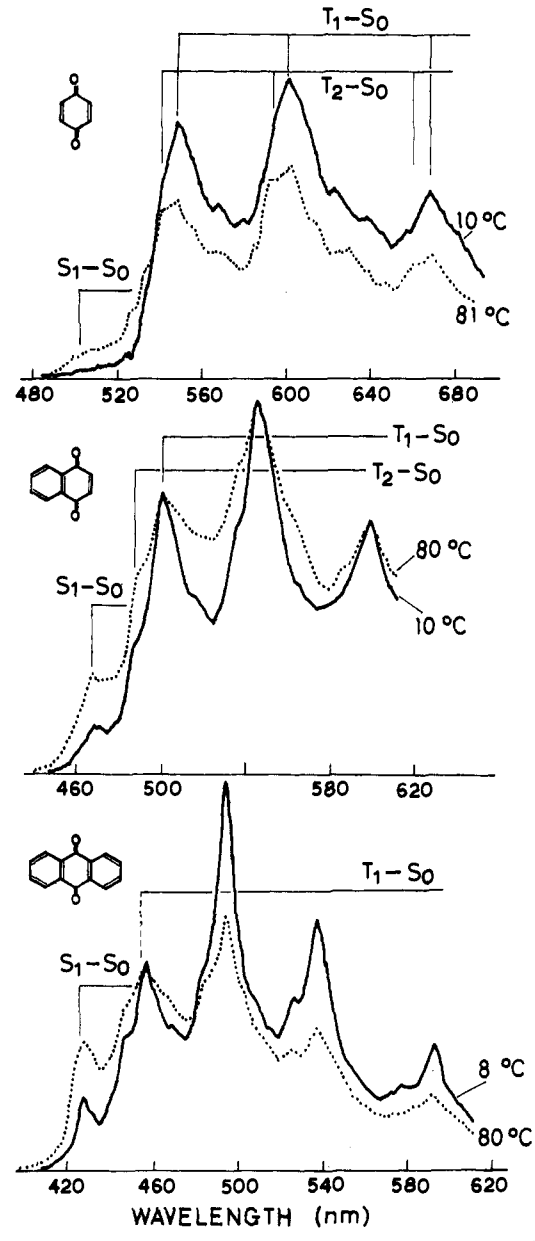

Figure 5. Emission spectra of Q[0,0], Q[1,0], and Q[1,1] in a degassed CCl_4 solution at two different temperatures.

In pure crystal the emitting state has been assigned as the lowest triplet state $^3B_{1g}$ which is located lower in energy than the ^3A_u state by 320 cm^{-1}.[47] The origin band in the $^3B_{1g} \rightarrow {}^1A_g$ phosphorescence is called LaPorte forbidden, but often becomes partially allowed by the crystal field.[43] In a naphthalene host, Q[0,0] exhibits the $^3B_{1g}$ phosphorescence with the missing origin, for which the b_{1u} vibrations are considered to play a dominant role in the intensity borrowing through vibronic spin-orbit coupling.[38,47,51] Further, in a neon host where Q[0,0] shows the dual phosphorescence from the $^3B_{1g}$ and ^3A_u states, two $^{1,3}(n,\pi^*)$ states are essentially degenerate with a $B_{1g}-A_u$ splitting of +64 cm^{-1} between the singlet and −11 cm^{-1} between the triplet states.[54]

In a degassed CCl_4 fluid solution, dual phosphorescence from the ^3A_u and $^3B_{1g}$ states has been observed in addition to the weak delayed fluorescence from $^1B_{1g}$.[55] The emission spectra of Q[0,0] in CCl_4 at different temperatures are shown in the first panel of Figure 5. The emission bands at 550 and 540 nm are regarded as the apparent ^3A_u and $^3B_{1g}$ phosphorescence origins, respectively, while a much weaker band near 500 nm as the fluorescence from $^1B_{1g}$ (S_1).[55] The fact that the relative intensity of the $T_2(^3A_u)$ and $S_1(^1B_{1g})$ emission to that of the $T_1(^3B_{1g})$ phosphorescence increases with temperature shows that these emitting states are in thermodynamic equilibrium.[55]

Although a number of emission spectral data have been reported for Q[0,0], the basic conception to understanding the data is that the spin−orbit-allowed ^3A_u state has much stronger oscillator strength than the forbidden $^3B_{1g}$ state which is located slightly lower in energy than ^3A_u. No emission has been observed for Q[0,0] in ordinary hydrocarbon matrices such as cyclohexane at low temperature. Stark effects (the effects of the electric field) on the S_1 and T_1 absorption,[41,60,61] on the phosphorescence spectra,[46] and on the phosphorescence microwave double reso-

Table 1. The ^1A_u, $^1B_{1g}$, ^3A_u, and $^3B_{1g}$ Origins[a] (cm^{-1}) of Q[0,0] Reported in Different Environments

environment	^1A_u	$^1B_{1g}$	^3A_u	$^3B_{1g}$	ref (year)
vapor		20031(a)	18682(a)		18 (1964)
			18683(m)		57 (1965)
			18723(m)		56 (1970)
			18685(m)	18370(m)	58 (1971)
		20031(m)	18682(m)		39 (1974)
	19991(x)	20045(x)			44 (1979)
	19998(x)	20052(x)	~18685(x)		45 (1988)
pure crystal	21003(a)[b]	20206(a)[b]	18942(a)[b]		34 (1956)
			18620(a)		36 (1967)
			18943(a)	18624(a)	47 (1970)
	20315(a)	20060(a)	18940	18620	22 (1972)
	20061(a)	20058(a)			39 (1974)
in neon	19984(x)	20047(x)	18665(m)	18654(m)	54 (1978)
in mixed crystals[c]					
Q[0,0]-d_4			18942(m)	18624(m)	47 (1970)
p-dibromobenzene				18373(m)	51 (1973)
Q[0,0]-d_4				18609(m)	38 (1975)
naphthalene				18163(m)	50 (1992)
in rigid glasses[c]					
propyl ether				18070(m)[b]	53 (1970)
di-*n*-propyl ether				18350(m,a)	33 (1970)
in fluid solutions[c]					
petroleum ether		~19950(a)[b]	~18550(a)[b]		34 (1956)
n-hexane			~18530(a)[b]		32 (1964)
perfluorohexane			18650(a)		58 (1971)
CCl_4		~20000(m,a)	~18500(m,a)	~18200(m,a)	55 (1984)

[a] a, m, and x in parentheses indicate that the state origins are determined from the absorption, emission and excitation spectra, respectively. [b] The symmetry is not specified. [c] All the data not shown.

nance (PMDR) signals[62] have been investigated for the single and mixed crystals. The result of the Stark effects on the T_1 absorption provided a strong support for the $^3B_{1g}$ assignment of T_1.[61] Further, it was confirmed that the strong vibronic interaction exists between $^1B_{1g}$ and ^1A_u as well as between $^3B_{1g}$ and ^3A_u to give double minimum potentials.[41,46,60-62] The LaPorte-forbidden $^3B_{1g}$ assignment of the T_1 state was confirmed also by the measurements of amplitude-modulated PMDR spectra,[51] thermally modulated phosphorescence spectra,[49] and optically detected magnetic resonance on the phosphorescence spectra.[48,51]

Table 1 summarizes the locations of the reported origins for the four low-lying states of Q[0,0] in different environments. All the available data show that there is general agreement so far as the locations of the ^1A_u, $^1B_{1g}$, and ^3A_u origins in the vapor phase are concerned. In pure crystal the experimental data support a model in which the ^3A_u and $^3B_{1g}$ states, and the $^1B_{1g}$ and $^3B_{1g}$ states are split by 320 and 440 cm^{-1}, respectively. Although in mixed crystals the location of the electronic origins depends somewhat on the host crystal, all the observed $^3B_{1g}$ states are considered to be located at energies below the ^3A_u states.

B. 1,4-Naphthoquinone

Absorption spectra of 1,4-naphthoquinone (Q[1,0]) have been obtained in the vapor phase,[5,6,42,63,64] in solutions,[5,6,27-30,40,65-74] in rigid glasses,[6,28] and in pure crystalline state[75,76] as well as in an oriented matrix or film.[77,78] The second curve in Figure 3a shows the absorption spectrum of Q[1,0] in hexane, in which the band at about 40 000 cm^{-1} ($\epsilon \sim 30\,000$) and that at 30 000 cm^{-1} ($\epsilon \sim 4000$) are both due to transitions to the $^1(\pi,\pi^*)$ states. Through the measurement of the absorption wavelength-dependent polarization of the phosphorescence,[28] it has been shown that each of the two $^1(\pi,\pi^*)$ absorption bands (the one ranging from 27 000 to 35 000 cm^{-1} and the other from 36 000 to 45 000 cm^{-1}) is due to the existence of two closely located $^1(\pi,\pi^*)$ states, $^1A_1$ and $^1B_2$. Polarization measurements using an oriented matrix or film also confirmed these assignments,[77,78] which have been supported by semiempirical calculations such as PPP[27,40,79] or CNDO/S-CI.[77,80] The weak visible absorption ($\epsilon \sim 60$) starting from 22 000 cm^{-1} corresponds to the transition to the $^1(n,\pi^*)$ state. The possibility for the appearance of two $^1(n,\pi^*)$ states in the absorption spectrum was pointed out,[75] but no unambiguous evidence has been obtained for this. A much weaker band ($\epsilon \sim 0.1$) at the red shoulder of the $^1(n,\pi^*)$ band is due to the transition to an $^3(n,\pi^*)$ state. This S → T band has been assigned as due to the transition to the $T_2(n,\pi^*)$ state which is considered to be located slightly higher in energy than $T_1(n,\pi^*)$.[6]

Emission of Q[1,0] has been observed in the vapor phase,[5,6,8,56,64,81,82] in crystalline state,[83] and in matrices[5,6,69,71,72,83-91] as well as in degassed fluid solutions.[6,87] The first curve in Figure 6 shows the emission spectrum of Q[1,0] in a rigid glass at 77 K, which has been identified as the phosphorescence from $T_1(n,\pi^*)$ on the basis of the spectral shape, lifetime, and position.[83,85] It is seen clearly that the spectrum shows the prominent feature in the C=O (b_2) stretching vibration with a frequency of 1670 cm^{-1}. Highly resolved phosphorescence spectra have been obtained in Shpolskii matrices at He temperature.[84,90]

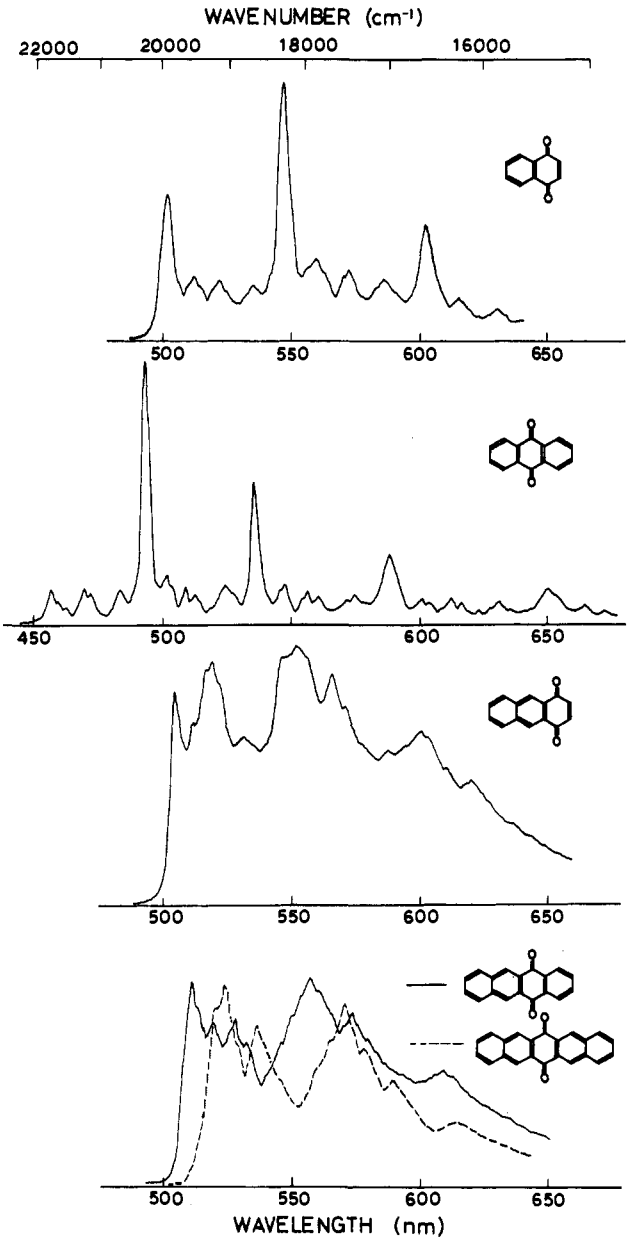

Figure 6. Phosphorescence spectra of Q[1,0], Q[1,1], Q[2,0], Q[2,1], and Q[2,2] in an isopentane–methylcyclohexane rigid glass at 77 K.

The vapor-phase emission spectrum has been obtained by several research groups,[5,56,81,82] but the early assignments of the emitting states were inconsistent with each other. More recently, it has been shown that the emission spectrum of Q[1,0] vapor consists of the dual phosphorescence from $T_1(n,\pi^*)$ and $T_2(n,\pi^*)$, and the delayed fluorescence from $S_1(n,\pi^*)$.[6] Further, it was demonstrated that low-pressure Q[1,0] vapor exhibits fluorescence from high vibrational levels of the singlet–triplet mixed state.[8] The emission spectrum of Q[1,0] static vapor is shown in the second panel of Figure 4, in which the emission from the three (n,π^*) states, T_1, T_2, and S_1, are clearly seen: The T_2 phosphorescence shows an allowed character, while the T_1 phosphorescence exhibits a sort of forbidden character.[6] In degassed fluid solutions containing no hydrogen atoms, Q[1,0] is reported to exhibit the T_1 and T_2 phosphorescence and thermally activated delayed fluorescence from S_1.[6,87] The emission spectra of Q[1,0] in CCl_4 at two different temperatures are shown as the second curves in Figure 5.

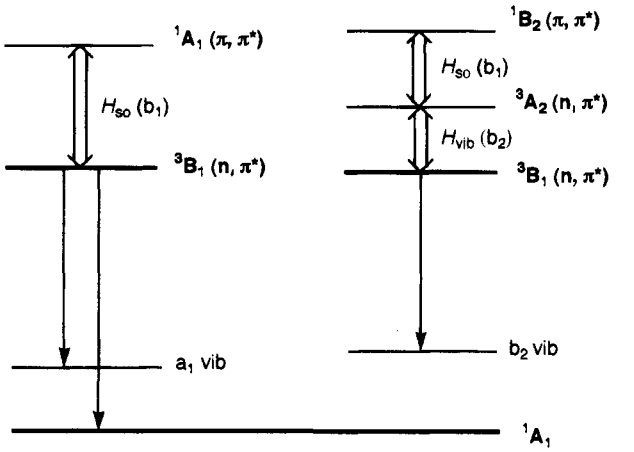

Figure 7. A scheme showing conceivable mechanisms for occurrence of the phosphorescence emission of Q[1,0].

It has been shown that the phosphorescence component of the emission in a rigid glass is polarized along the z-axis in the region near the origin, while it is polarized along y-axis in the longer wavelength region.[84,85] However, the symmetry of the T_1 state could not be determined unambiguously only from these experiments. Galaup et al.[76] have investigated the S–T absorption spectrum of the single crystal in electric and magnetic fields and showed that the T_1 state is regarded as a superposition of the two $^3(n,\pi^*)$ states, with the contribution of the $^3B_1$ state (in the coordinate system treated here) being predominant ($|T_1\rangle = |^3B_1\rangle - 0.08|^3A_2\rangle$). On the basis of the vibrational modes appearing in the phosphorescence spectrum, Strokach et al. have assigned T_1 as $^3B_1$ and proposed mechanisms for the occurrence of the $^3B_1 \rightarrow {}^1A_1$ transition (Figure 7):[90] The direct spin–orbit interaction between $^1A_1$ and $^3B_1$ is responsible for the appearance of the a_1 vibrational bands in the phosphorescence, while for the appearance of the b_2 bands, the conceivable mechanism is the spin–orbit interaction between $^1B_2$ and $^3A_2$ involving the vibronic interaction between the intermediate $^3A_2$ and $^3B_1$ states through the b_2 vibration. Itoh has suggested, through the observation of the temperature dependence of the vapor-phase emission and group theoretical and simple molecular orbital considerations, that the T_1 and T_2 states of Q[1,0] vapor are, respectively, $^3B_1$ and $^3A_2$.[6] All of these investigations seem to support a model in which the T_1 state is $^3B_1$ (direction of x-axis) and the T_2 state is $^3A_2$. The observation that the $T_1(^3B_1)$ phosphorescence in the vapor phase exhibits a sort of forbidden character also supports the vibronic spin–orbit interaction as a dominant mechanism for the $^3B_1 \rightarrow {}^1A_1$ transition (Figure 4).[6]

Table 2 summarizes the observed origins of the low-lying states of Q[1,0] in different environments. More recent analyses of the vapor-phase emission indicated that the $^3A_2$ and $^3B_1$ origins are located at 20 475 and 20 295 cm^{-1}, respectively.[6] Supersonic jet experiments of Q[1,0] vapor are needed in order to get a more accurate picture of the electronic states. There is general agreement concerning the location of the T_1 origin in rigid glasses at 77 K and in mixed

Table 2. The Origins[a] (cm^{-1}) for the Lower Lying Electronic States of Q[1,0] Reported in Different Environments

environment	$^1A_2/^1B_1$[d]	$^3A_2$	$^3B_1$	ref (year)
vapor	21945(m)[b]	18782(m)[b]		81 (1967)
	23161(a)[b]	21944(a)[b]		63 (1968)
	22163(m)/21974(m)[b]			56 (1970)
		19990(a,m)[b]		64 (1973)
	21940(m,a)[b]	20475(m)	20295(m)	6 (1987)
pure crystal	21932(a)/21789(a)[b]			75 (1978)
			20238(a)	76 (1978)
in mixed crystals[c]				
hexane			~19940(m)[b]	91 (1978)
n-hexane			20158(m)[b]	84 (1984)
in rigid glasses[c]				
EPA			20160(m)[b]	72 (1967)
methylcyclohexane			~19820(m)[b]	83 (1967)
PM			19950(m)[b]	84 (1984)
methylcyclohexane	~21850(a)[b]			6 (1987)
in fluid solutions[c]				
freon	~21350(m)[b]		~19500(m)[b]	87 (1971)
isopentane	~21850(a)[b]	~20500(a)[b]		5 (1979)
CCl_4	~21400(m,a)[b]	~20400(m,a)	~20000(m,a)	6 (1987)

[a] a, m, and x in parentheses are the same as in Table 1. PM denotes an isopentane–methylcyclohexane mixture. [b] The symmetry is not specified or the symmetry assignment is considered to be incorrect. [c] All the data not shown. Note that site bands often appear for mixed crystalline samples. [d] With Q[1,0], each of the two $^1(n,\pi^*)$ states has not been specified.

crystals at He temperature. In pure crystal, the lowest triplet state was assigned primarily as $^3B_1$ with the origin at 20238 cm^{-1}.[76] In a degassed CCl_4 fluid solution, Q[1,0] exhibits the dual phosphorescence from the T_1 and T_2 states in addition to the S_1-delayed fluorescence.[6] Although the $^1(n,\pi^*)$ state has been identified clearly in the absorption, excitation, and delayed fluorescence spectra, unambiguous symmetry determination ($^1A_2$ or $^1B_1$) and identification of the two $^1(n,\pi^*)$ states have not been reported.

C. 9,10-Anthraquinone

The electronic states and spectra of 9,10-anthraquinone (Q[1,1]) were often compared with those of the simplest D_{2h} quinone, Q[0,0]. Although a review on the spectroscopy and photochemistry of the derivatives of Q[1,1] was published recently,[92] a number of spectroscopic data have been obtained solely for the parent molecule. Absorption spectra of Q[1,1] have been obtained in the vapor phase,[93–98] in solution,[28,29,40,66,67,72,74,79,99–106] in pure[75,103,107–113] and mixed crystallline states,[114,115] and in a rigid glass[28,112] as well as in a stretched film or polymer.[104] The third curve in Figure 3a shows the absorption spectrum of Q[1,1] in hexane. The bands starting from 37 000 cm^{-1} and those starting from 30 000 cm^{-1} are both due to transitions to the $^1(\pi,\pi^*)$ states. The weak visible absorption ($\epsilon \sim 100$) with the apparent origin at 23 750 cm^{-1} corresponds to the transition to the lowest $^1(n,\pi^*)$ state with the $^1B_{1g}$ symmetry. Unlike Q[0,0] and Q[1,0], the S → T absorption band cannot be seen clearly for Q[1,1] in room temperature solvents,although it has been observed for the pure and mixed crystals.[103,108,110,111,114] The T_1 state was initially assigned as $^3A_u(n,\pi^*)$,[112,116] but the $^3B_{1g}(n,\pi^*)$ assignment of T_1 has been supported by a number of research groups through the measurements of the highly resolved phosphorescence and absorption spectra of the pure and mixed crystals.[108–111,114,116–121] For example, a weak absorption band at 22 153 cm^{-1} of the pure crystal has been assigned as the origin of the symmetry-forbidden transition to the $^3B_{1g}$ state by means of combined Stark–Zeeman experiments.[110] Further, the two $^3(n,\pi^*)$ states, ^3A_u and $^3B_{1g}$, have been identified in the absorption spectrum of the pure crystal.[109]

Emission or excitation spectra of Q[1,1] have been obtained in pure[108] and mixed crystalline states,[88,109,111,114,115,117–125] in rigid glasses,[72,85,102,112,123,126–129] and in degassed fluid solutions[102,129] as well as in the vapor phase.[56,96,97,102,116,130–133] The $T_1(^3B_{1g})$ phosphorescence spectrum of Q[1,1] in a rigid glass at 77 K is shown in the second panel of Figure 6. It is clearly seen that the spectrum exhibits a sort of forbidden character, i. e., the origin band is extremely weak or missing. This character is more pronounced for the phosphorescence spectra of Q[1,1] doped in appropriate Shpolskii matrices, in which the inversion center of the molecule is retained. However, when the molecule is distorted from the D_{2h} symmetry by the crystal field or by attachment of a substituent onto the aromatic subsystem, the origin band can have appreciable intensity.[1,79,111,118] Although a number of the highly resolved $^3B_{1g}$ phosphorescence spectra in Shpolskii matrices have been reported, in some cases the assignments of the vibrational bands were inconsistent with each other, presumably due to the existence of multiple sites. In order to overcome this situation, Murao and Azumi have measured the spin-sublevel phosphorescence spectra originating from individual sites utilizing a PMDR technique.[121] The observed x, y, and z spin-sublevel spectra were shown to have, respectively, vibronic bands due to only b_{3u}, b_{2u}, and b_{1u} vibrations. That is, the wavenumber of the vibronic bands, $\nu(x, y,$ or $z)$, in the three spin-sublevel phosphorescence are given by, $\nu(x, y,$ or $z) = \nu(0) - \nu(b_{3u}, b_{2u},$ or $b_{1u}) - n \times \nu_3 - m \times \nu_{12}$, where n, $m = 1$ or 0, ν_3 and ν_{12} are the frequencies of totally symmetric vibrations (with the

Table 3. The Origins[a] (cm^{-1}) for the Lower Lying Electronic States of Q[1,1] Reported in Different Environments

environment	^1A_u	$^1B_{1g}$	^3A_u	$^3B_{1g}$	ref (year)
vapor		23730(m)/23657(m)[b]			56 (1970)
		23750(m)[b]		21750(m)[b]	130 (1982)
		~23700(m,a)[b]		22030(m)	102 (1986)
pure crystal		23559(a)[b]			75 (1956)
				22154(a)	108 (1975)
		23562(a)	22560(a)	22150(a)	109 (1975)
				22153(a)	110 (1976)
		23563(a)		22153(x)	111 (1979)
in mixed crystals[c]					
Q[1,1]-d_8				22156(m)	109 (1975)
n-heptane				21768(m)	119 (1977)
n-pentane	27196(x)?	23217(x)			111 (1979)
n-hexane		23198(x)			111 (1979)
heptane			~22100	21755(m, x)	114 (1979)
CCl_4				21760(m, x)	114 (1979)
n-hexane				21783(m)	120 (1979)
in rigid glasses[c]					
EPA				21980(m)[b]	72 (1967)
freon				~21900(m)[b]	129 (1971)
PM				~21950(m)	102 (1986)
in fluid solutions[c]					
freon		~23360(m)[b]		~21930(m)[b]	87 (1971)
cyclohexane		~23600(a)[b]			28 (1974)
CCl_4		~23400(m,a)[b]		~21800(m)	102 (1986)

[a] a, m, and x in parentheses are the same as in Table 1. See Table 2 for PM. [b] The symmetry is not specified or the symmetry assignment is considered to be incorrect. [c] All the data not shown. Note that site bands often appear for mixed crystalline samples.

subscript numbers being due to Mulliken convention), $\nu(0)$ is that of the missing $^3B_{1g}$ origin, and $\nu(b_{3u}, b_{2u}$, or $b_{1u})$ represents, respectively, that of one of the b_{3u}, b_{2u}, or b_{1u} vibrations. It was also suggested that the x, y, and z spin-sublevel phosphorescence gain their intensities mainly through the vibronic spin–orbit coupling involving the vibronic coupling between $^1B_{2g}(\sigma,\pi^*)$ and $^1B_{1u}(\pi,\pi^*)$, $^3B_{1g}(n,\pi^*)$ and $^3B_{3u}(\sigma,\pi^*)$, and $^3B_{1g}(n,\pi^*)$ and $^3A_u(n,\pi^*)$, respectively (see also Appendix A).[121]

In degassed fluid solutions containing no hydrogen atoms, Q[1,1] exhibits the phosphorescence from $T_1(n,\pi^*)$ and the delayed fluorescence from $S_1(n,\pi^*)$.[102,129] The emission spectra of Q[1,1] in a degassed CCl_4 fluid solution at two different temperatures are shown in the third panel of Figure 5. It is seen that the weakness of the T_1-phosphorescence origin is partly retained also in a fluid solution.

Several emission spectral data have been reported for Q[1,1] static vapor, but the early assignments, and in some case the spectrum itself, were inconsistent with each other. For example, the spectrum reported in ref 130 consists of several sharp peaks at high temperature and the spectral feature is somewhat different from those reported previously. It is unlikely that large polyatomic molecules like Q[1,1] exhibit such sharp emission peaks at temperatures as high as 180 °C, and presumably involvement of some other signal such as scattering must be considered. Other reported vapor-phase emission spectra show essentially the same spectral feature among each other. The emission spectrum of Q[1,1] vapor is shown in the third panel of Figure 4. This emission has been shown to consist mostly of the T_1 phosphorescence with the invisible origin at ~22 030 cm^{-1} and of the S_1-delayed fluorescence, with the apparent origin at ~23 700 cm^{-1}.[102] Borisevich has reported the delayed fluorescence resulting from the multiphoton excitation of Q[1,1] vapor,[131,133] and Emel'yanov et al. have shown that at low pressure the emission consists of the phosphorescence and direct fluorescence accompanied by delayed fluorescence.[132]

In Table 3 the locations of the observed low-lying electronic origins are summarized for Q[1,1] in different environments. There is general agreement concerning the location of the $^1B_{1g}$ and $^3B_{1g}$ origins of the pure crystal. Although the emission spectrum of Q[1,1] vapor at high total pressure is considered to consist of the T_1 phosphorescence and S_1 delayed fluorescence, accurate determination of the state origins may be difficult, since the emission spectrum turns out to be extremely broad at high temperature. Supersonic jet experiments of Q[1,1] are needed as in the case of Q[1,0]. The four low-lying (n,π^*) states, $^{1,3}A_u$ and $^{1,3}B_{1g}$, are expected to be located in a narrow range 21 000~24 000 cm^{-1}, but all of them have not been identified unambiguously.

D. Other Higher Linear Para Quinones

The reported absorption and emission spectral data for linear para acenequinones other than Q[0,0], Q[1,0], and Q[1, 1] are significantly limited. In para quinones of the type Q[m,n] with $m = 2$, and $n = 0$, 1 and 2, the lowest $^1(n,\pi^*)$ absorption band is observed as a weak shoulder on the red side of the lowest $^1(\pi,\pi^*)$ band, with the apparent origins at 22 100, 24 050, and 24 150 cm^{-1}, respectively, for Q[2,0], Q[2,1], and Q[2,2] in nonpolar hydrocarbons (Figure 3, parts a and b). The ϵ values at the origin of the $^1(n,\pi^*)$ bands of these molecules are large as compared with those of other smaller quinones as

well as other aromatic carbonyl compounds; 220, 370, and 400 for Q[2,0], Q[2,1], and Q[2,2], respectively. Although convincing evidence has not been given identifying these weak bands as due to the n → π* transition, it is almost certain that these are the $^1(n,\pi^*)$ absorption bands based on the fact that these bands disappear upon addition of a small amount of alcohol or acetic acid into the solution.[15,28] The comparatively large ε values of these $^1(n,\pi^*)$ bands are most probably due to close proximity to the upper $^1(\pi,\pi^*)$ states from which the intensity is borrowed.[15] The apparent origins of the first $^1(\pi,\pi^*)$ absorption band of Q[2,0], Q[2,1], and Q[2,2] are seen, respectively, at 23 800, 25 250 and 25 600 cm^{-1} in nonpolar hydrocarbons at room temperature (Figure 3, parts a and b).

The emission spectra of Q[2,1] and Q[2,2] were obtained first by Zander,[72] but Shcheglova and Lesnenko[134] criticized the assignments by Zander and stated that the T_1 state is of (π,π^*) type. The polarization spectra of the phosphorescence of Q[2,0], Q[2,1], and Q[2,2] were measured by Novak et al.[28] and by Nepras and Novak[85] who also treated the emission as originating from the $T_1(\pi,\pi^*)$ state. The phosphorescence spectra of Q[2,0], Q[2,1], and Q[2,2] in a rigid glass at 77 K are displayed in Figure 6. On the basis of the spectral shape and position as well as the lifetime, the observed emission is safely attributed to the $T_1(\pi,\pi^*)$ phosphorescence with the apparent origins at 19 740, 19 160, and 18 920 cm^{-1}, respectively, for Q[2,0], Q[2,1], and Q[2,2].

With Q[3,0], Q[3,2], and Q[3,3] both of the lowest singlet and triplet (π,π^*) states are located below the lowest excited $^1(n,\pi^*)$ state and the fluorescence from $^1(\pi,\pi^*)$ has been observed.[72,135] In solution the apparent origins of the first $^1(\pi,\pi^*)$ absorption bands are observed at ~20 800, ~22 000, and ~21 700 cm^{-1}, respectively, for Q[3,0], Q[3,2], and Q[3,3] (Figure 3b).[72,135] The location of the lowest $^3(\pi,\pi^*)$ state has not been determined for these molecules.

IV. Quantum Chemical Calculations of the Excited Electronic States

Transition energies, polarization, and oscillator strengths have normally been used to check the calculated excited-state wave functions of para quinones. The excitation energies of Q[0,0] have been calculated mostly with semiempirical methods such as PPP,[12,13,28,40,79,136-150] CNDO,[24,80,150-158] MIM,[159] INDO,[150,160] MINDO,[161] MS-Xα,[162] HAM,[163] or others.[164,165] These semiempirical outputs may not be compared directly with each other, since these were obtained using different parameters, degrees of CI (configuration interaction) and molecular geometries. One thing in common with these calculations is the ordering of the excited singlet states in an UV–vis region, $^1B_{1g}(n,\pi^*) < {}^1A_u(n,\pi^*) < {}^1B_{3g}(\pi,\pi^*) < {}^1B_{1u}(\pi,\pi^*)$ < etc., although the state ordering, $^1B_{1g} < {}^1A_u$, is in conflict with the recent observations for Q[0,0] vapor. Further, the calculated energy differences between the two $^1(n,\pi^*)$ states are apparently large as compared with the experimental values. The excitation energies in MO treatments has been improved with increasing the degree of incorporated CI.[80] The observed excitation energies were well reproduced by the HAM/3 (hydrogenic atoms in molecules) method,[163] with less success by CNDO/S for Q[0,0], but Jacques et al. reproduced them comparatively well by CNDO/S with appropriate choice of parameters and the degree of CI.[157] The CNDO/S-CI outputs by Jacques et al., for example, are $^1B_{1g}$ = 2.46 (2.486); ^1A_u = 2.60 (2.479); $^1B_{3g}$ = 4.13 (4.05); and $^1B_{1u}$ = 5.10 eV(5.0 eV), with the experimental values for Q[0,0] vapor shown in parentheses.[157] Masmanidis et al. have evaluated the matrix elements for direct spin–orbit coupling using CNDO/S wave functions for Q[0,0].[153] The oscillator strength for the $^3A_u \leftarrow {}^1A_g$ transition was shown to be the largest among the transitions from ^1A_g to four closely-located triplet states, ^3A_u, $^3B_{1u}$, $^3B_{1g}$, and $^3B_{3g}$.

Wood was probably the first to report the ab initio excitation energies of Q[0,0] (12-atom molecule) using minimal basis sets with single excitation CI.[166] Although ab inito calculations are considered to be more theoretical in the sense that they contain practically no parameters, the reproducibility of the excitation energies is generally poor as compared with semiempirical results. As in the case of semiempirical outputs, the ab initio 1^1B_{1g} energies are slightly lower than the 1^1A_u energies both for singlet and triplet states. Further, in most cases the $^3B_{1u}$ (π,π^*) state is shown to have a lower energy than the $^3(n,\pi^*)$ states, which conflicts with the observations. Reduction in the ab initio excitation energies has been achieved by incorporating higher order correlation effects such as quadruple excitations or multireference CI. The ab initio outputs for Q[0,0] by Ha, obtained with multireference single and double excitations CI, for example, are[167] $^3B_{1u}$ = 2.46; $^3B_{1g}$ = 2.72; ^3A_u = 2.79; $^1B_{1g}$ = 3.04; ^1A_u = 3.07; $^1B_{3g}$ = 4.49; and $^1B_{1u}$ = 6.11 eV. These results may predict the existence of the $^3B_{1u}(\pi,\pi^*)$ state in the same energy range of the $^{1,3}(n,\pi^*)$ states. Martin et al. have shown that a BV model involving the broken symmetry solutions to the Hartree–Fock equations provided reasonably accurate excitation energies for the $^{1,3}(n,\pi^*)$ states of Q[0,0].[168,169] Ab initio calculations of Q[0,0] up to 1983 were reviewed by Ball and Thomson who pointed out the danger of using the ground state geometry for the excited-state calculations.[170]

The calculations for Q[1,0] have been carried out all with semiemipirical methods such as PPP,[13,28,40,79,140,141,144,147,149,153,171] MIM (molecules-in molecules) method,[172] CNDO,[80,77,171,173] or INDO.[160] For example, the singlet energies obtained using CNDO/S-CI by Kuboyama et al. are[80] $1^1B_1(n_-,\pi^*)$ = 2.601 (2.72); $1^1A_2(n_+,\pi^*)$ = 2.609; 2^1A_1 = 3.804 (~3.8); 1^1B_2 = 4.116 (~3.8); 2^1B_2 = 4.866 (~5.1); and 3^1A_1 = 5.199 eV (~5.1 eV), with the experimental values shown in parentheses. There is general agreement in the semiemprical outputs that each of the two $^1(\pi,\pi^*)$ absorption bands of Q[1,0] (the one ranging from 27 000 to 35 000 cm^{-1} and the other from 36 000 to 45 000 cm^{-1}) is due to the existence of two nearly degenerate $^1A_1$ and $^1B_2$ states.

Although the excitation energies of Q[1,1] have been calculated semiempirically,[12,13,28,40,79,80,101,140,141,149,173-176] the only exception is the ab initio calculation reported by Petke et al.[177] who have discussed possible mechanisms of the S_1–T_1 intersystem crossing and intensity borrowing in phosphorescence in terms of the first- and second-

order spin–orbit and vibronic perturbations of the singlet and triplet states. They have obtained the following energies for Q[1,1]:[177] 1^3B_{1g} = 2.488 (2.732); 1^3A_u = 2.624; 1^1B_{1g} = 2.768 (2.939); 1^3B_{1u} = 2.878; 1^1A_u = 2.909; 1^1B_{2u} = 3.808 (3.72); 1^1B_{1u} = 4.482 (4.56); and 2^1B_{2u} = 4.916 eV (4.92 eV), with the plausible experimental values shown in parentheses. The excitation energies have been calculated also for higher quinones such as Q[2,0], Q[2,1] or Q[2,2], all with semiempirical methods.[140,149,173,178] Olbrich et al. have obtained the excitation energies of these molecules with modified CNDO/S-CI and shown that the $^{1,3}(n,\pi^*)$ state energies and the separations depend only slightly on the size of quinones.[173]

Quantum chemical outputs can provide us information on the orbital arrangements, the energy levels of the optically masked states such as $^3(\pi,\pi^*)$, and the excited-state geometry, which we can hardly obtain empirically. In MO treatments, an appropriate choice of geometry for the excited and ground states and basis sets as well as incorporation of extensive CI may be the key to obtaining more reliable results.

V. Excited-State Ordering and Emitting States

The dependence of electronic excitation energies on quinone size is of special interest. Hartmann and Lorenz first showed that the carbonyl group in quinones interrupted the π-electron delocalization and that the position of the first singlet $\pi \rightarrow \pi^*$ transition was determined by the size of the aromatic subsystem (m or n in Q[m,n]).[66] Nepras and Titz have attempted to provide a quantitative interpretation for Hartmann's observation using a PPP method.[12] The $^1(\pi,\pi^*)$ electronic spectra have been interpreted in terms of the local and charge-transfer transitions of the aromatic subsystem. They stated that the lowest $^1(\pi,\pi^*)$ state energies in acenequinones depend not only on the size of the larger aromatic subsystem but also on the size of smaller one.[12] Kunavin and Shvekhgeimer reported that the $^{1,3}(n,\pi^*)$ state energies of dicarbonyl compounds depend both on the presence of vinyl groups conjugated with carbonyl groups and on the mutual position of carbonyl groups in a molecule.[106] As is seen in Figure 8, the energy levels of the lowest

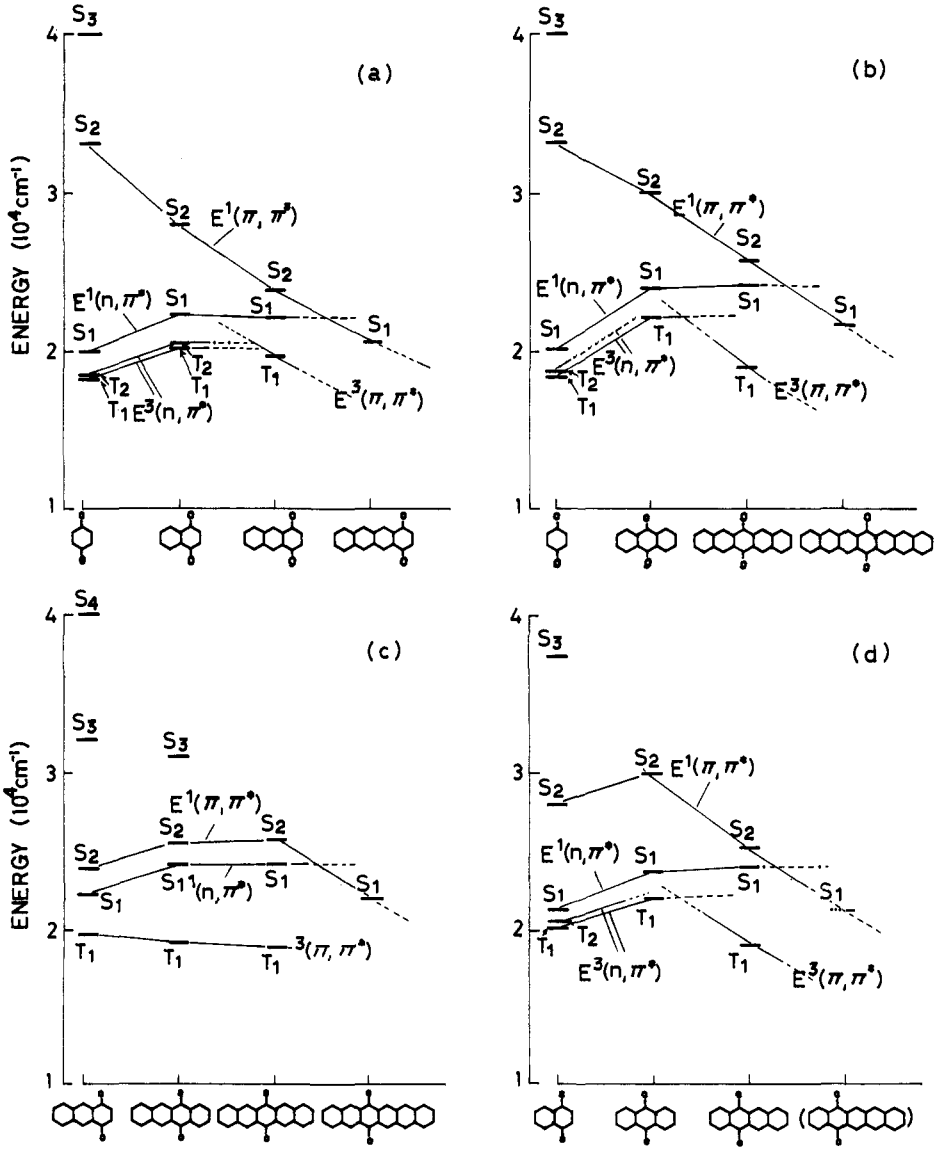

Figure 8. Diagrams showing the variation of the excited-state levels upon a systematic change of the chemical structure of linear para acenequinones.

$^1(\pi,\pi^*)$ state, $E^1(\pi,\pi^*)$, are almost in accordance with Hartmann's rule:[66] When m is increased successively from 0 in the systems Q[m,0], $E^1(\pi,\pi^*)$ shows a monotonous decrease (Figure 8a); the situation is almost the same for the systems Q[m,m] (Figure 8b); when n is increased successively from 0 in the systems Q[2,n], $E^1(\pi,\pi^*)$ shows an abrupt decrease on going from $n = 2$ to $n = 3$ (Figure 8c); and the situation is almost the same for the systems Q[1,n], for which $E^1(\pi,\pi^*)$ shows an abrupt decrease on going from $n = 1$ to $n = 2$ (Figure 8d).

It is recognized from the energy-level diagrams in Figure 8 that $E^1(\pi,\pi^*)$ is determined primarily by the number "m" in Q[m,n] ($m \geq n$), while the location of the lowest $^1(n,\pi^*)$ states, $E^1(n,\pi^*)$, is almost independent of the size of the aromatic subsystem,[173] although closer inspection of Figure 8 reveals a slight change of $E^1(n,\pi^*)$ depending on the quinone size. The values for $E^1(\pi,\pi^*)$ and $E^1(n,\pi^*)$ of Q[m,n] ($m \geq n$) can be expressed empirically by very simple expressions of the forms[15]

$$E^1(\pi,\pi^*) = 10\,000 + 50\,000 \times (1 + k/10)/(m + 2)\ (\mathrm{cm}^{-1}) \quad (1a)$$

$$E^1(n,\pi^*) = 20\,000 \times (1 + k/10)\ (\mathrm{cm}^{-1}) \quad (1b)$$

where k is a parameter; $k = 0$ for Q[0,0], $k = 1$ for Q[m,0] with $m \neq 0$, and $k = 2$ for Q[m,n] with m, $n > 0$. The term $50\,000/(m + 2)$ in eq 1a corresponds to an approximate variation of the lowest $^1(\pi,\pi^*)$ level of aromatic subsystem with varying the polyacence subsystem size, although the nature of the lowest excited singlet state of linear polyacenes changes from $^1L_b(\pi,\pi^*)$ to $^1L_a(\pi,\pi^*)$, on going from naphthalene to anthracence. On the other hand, $E^1(n,\pi^*)$ is determined basically by whether or not the aromatic subsystem exists next to parent p-benzoquinone. Equations 1a and 1b allow the reliable estimation of the low-lying excited singlet energies of the present systems. Considering the nearly fixed energy separations between the singlet and triplet states with the same electronic configuration, similar equations can be derived also for the triplet levels.[15]

The emitting states of the nine quinones are summarized in Table 4. The emission properties are closely related to the ordering and nature of the excited states, according to El-Sayed's selection rule and Plotnikov's classification.[177,179,180] All the linear para acenequinones belong to one of the three types displayed in Figure 9 depending on the excited-state ordering. In quinones of the type Q[m,n] with m, $n = 0$ or 1, both of the lowest singlet and triplet (n,π^*) states are located below the lowest excited $^1(\pi,\pi^*)$ state (case a in Figure 9). Hence, these molecules exhibit the $^3(n,\pi^*)$ phosphorescence and $^1(n,\pi^*)$ fluorescence, with the latter emission being due to thermal activation of the $^3(n,\pi^*)$ state; the lowest $^3(\pi,\pi^*)$ state is presumably located between the lowest $^3(n,\pi^*)$ and $^1(n,\pi^*)$ states for Q[1,1]. In the systems of the type Q[m,n] with $m = 2$, and $n = 0$, 1, and 2, the singlet and triplet (n,π^*) states are both located between the $^1(\pi,\pi^*)$ and $^3(\pi,\pi^*)$ states (case b in Figure 9). Hence, these molecules exhibit phosphorescence from the $^3(\pi,\pi^*)$ state in rigid matrices at 77 K. Q[3,0] exhibits only fluorescence from the $^1(\pi,\pi^*)$ state,[135] indicating that the $^1(n,\pi^*)$ state, and probably the $^3(n,\pi^*)$ state also, lies above the lowest $^1(\pi,\pi^*)$ state (case c in Figure 9). The situation is exactly the same for Q[3,2] and Q[3,3] which exhibit the fluorescence from $^1(\pi,\pi^*)$.[72] Although the absorption and emission spectral data have not been obtained for other higher systems, we can expect that quinones of the type Q[m,n] with $m > 3$ exhibit fluorescence from the lowest $^1(\pi,\pi^*)$ state and that both of the lowest $^{1,3}(\pi,\pi^*)$ states are located well below the lowest $^{1,3}(n,\pi^*)$ states.

Table 4. Reported Emitting States of Linear Para Acenequinones

molecule	vapor	in rigid glasses[a]	in fluid solutions[b]	pure crystal
Q[0,0]	$S_1(n,\pi^*)$, $T_2(n,\pi^*)$	*c*	$S_1(n,\pi^*)$, $T_2(n,\pi^*)$, $T_1(n,\pi^*)$	$T_1(n,\pi^*)$
Q[1,0]	$S_1(n,\pi^*)$, $T_2(n,\pi^*)$, $T_1(n,\pi^*)$	$T_1(n,\pi^*)$	$S_1(n,\pi^*)$, $T_2(n,\pi^*)$, $T_1(n,\pi^*)$	*d*
Q[1,1]	$S_1(n,\pi^*)$, $T_1(n,\pi^*)$	$T_1(n,\pi^*)$	$S_1(n,\pi^*)$, $T_1(n,\pi^*)$	$T_1(n,\pi^*)$
Q[2,0]		$T_1(\pi,\pi^*)$	$S_1(n,\pi^*)$[e]	
Q[2,1]		$T_1(\pi,\pi^*)$		
Q[3,0]			$S_1(\pi,\pi^*)$	
Q[2,2]		$T_1(\pi,\pi^*)$		
Q[3,2]			$S_1(\pi,\pi^*)$	
Q[3,3]			$S_1(\pi,\pi^*)$	

[a] In hydrocarbon glasses at 77 K. [b] In degassed CCl_4 at room temperature for Q[0,0], Q[1,0], Q[1,1], and Q[2,0]. In degassed fluid solutions containing hydrogen atoms; smaller para quinones normally exhibit no emission. [c] In some matrix such as naphthalene or propyl ether at low temperature, Q[0,0] was reported to show the emission from $T_1(n,\pi^*)$ and/or $T_2(n,\pi^*)$. [d] The emission of microcrystalline Q[1,0] is considered to be originating from the aggregated forms. [e] Quite recently, the emission which can be regarded as originating from $S_1(n,\pi^*)$ has been observed for Q[2,0] in carefully degassed CCl_4 at room temperature. (Itoh, T.; Yamaji, M.; Shizuka, H. Unpublished data.) This emission is most probably due to the thermal population of $T_1(\pi,\pi^*)$ and/or $T_2(n,\pi^*)$.

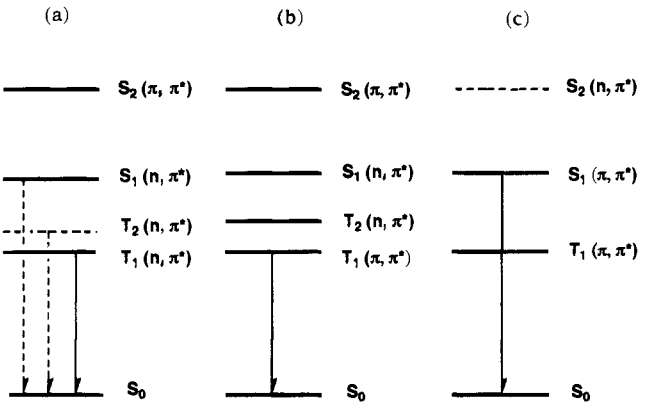

Figure 9. A scheme showing the state ordering and emitting states for linear para acenequinones.

VI. Photophysical Properties

A. Photophysics in the Condensed Phases

In the condensed phases such as in fluid solutions or in rigid matrices, a molecule suffers sufficient collisions during the lifetime of the excited states. Hence, it is relaxed ultimately to lower vibrational levels of the lowest excited states and normally

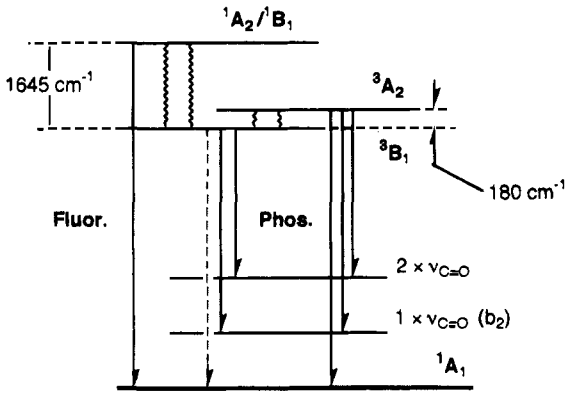

Figure 10. A scheme showing thermal population and occurrence of the dual phosphorescence and delayed fluorescence of Q[1,0] static vapor in the presence of an added foreign gas.

exhibits the emission only from the levels near the origin of the lowest excited singlet or triplet state. The generalization of this observation is now referred to as Kasha's rule. Also in the static vapor at high total pressure (e.g., ~10^2 Torr), a molecule suffers sufficient collisions during the lifetime, so that in general the photophysical behavior is almost the same as that observed in the condensed phases. As was mentioned, a sort of anti-Kasha emission has been observed for Q[0,0] and Q[1,0]. This emission property is due to the characteristic electronic structure of para quinones in which two or three emitting states are closely located to each other.

The scheme showing the occurrence of the thermal population and delayed emission is illustrated in Figure 10 for Q[1,0] vapor as an example. When more than two emitting states are in thermodynamic equilibrium, the quantum yield ratio of the emission from the upper state to that from the lower state is proportional to the value, $\exp(-\Delta E/kT)$, where k is the Boltzmann constant, T is absolute temperature, and ΔE is the energy separation between the two emitting states. In fact, ΔE values obtained from the temperature dependence of the quantum yield ratios agree well with those obtained spectroscopically for Q[0,0], Q[1,0], and Q[1,1].[5,6,9,55,87,102,129] Of course, at much lower temperatures where the Boltzmann factor is significantly small, the emission originates only from the lowest triplet state.

The intrinsic phosphorescence lifetime τ^0 is normally obtained by the relation

$$\tau^0 = \tau^{obs}/\Phi_P \quad (2)$$

where τ^{obs} and Φ_P stand for the observed phosphorescence lifetime and quantum yield, respectively. With Q[1,0] in a rigid glass matrix at 77 K, for example, eq 2 can apply directly to obtain the value for τ^0, since the T_1 population yield is considered to be almost unity. The value for τ^{obs} of Q[1,0] in methylcyclohexane at 77 K is reported to be 5×10^{-4} s,[6] with Φ_P of 0.1. Hence, τ^0 of the $T_1(n,\pi^*)$ state is estimated to be 5×10^{-3} s,[6] which is a reasonable value for the radiative lifetime of the $^3(n,\pi^*)$ state. However, the relationship between the observed and intrinsic lifetime is somewhat complicated for Q[1,0] vapor at high total pressure, since the emission originates from three different electronic states in thermal equilibrium. In this case, the thermally averaged lifetime is approximately expressed by,[6]

$$\tau^{obs} = [k(T_1) + k(T_2)\exp[-\Delta E(T_2-T_1)/kT] + k(S_1)\exp[-\Delta E(S_1-T_1)/kT]]^{-1} \quad (3)$$

where $k(i) = k_r(i) + k_{nr}(i)$, with $k_r(i)$ and $k_{nr}(i)$ denoting, respectively, the radiative and nonradiative rate constants of the state i. As is indicated by eq 3, the observed decay curves cannot be multiexponential, although the emission originates from the three electronic states with different radiative rate constants. In fact, the observed emission decay curves of Q[1,0] vapor in the presence of a buffer gas showed a single exponential decay,[5] with the lifetime of 84 μs and the relative quantum yields of 0.7, 1, and 0.2, respectively, for the T_1, T_2, and S_1 emission at 80 °C.[6,8] Since the quantum yield ratios, $\Phi_P(T_2)/\Phi_P(T_1)$ and $\Phi_F(S_1)/\Phi_P(T_1)$, are expressed by

$$\Phi_P(T_2)/\Phi_P(T_1) = k_r(T_2) \times \exp[-\Delta E(T_2-T_1)/kT]/k_r(T_1) \quad (4a)$$

$$\Phi_F(S_1)/\Phi_P(T_1) = k_r(S_1) \times \exp[-\Delta E(S_1-T_1)/kT]/k_r(T_1) \quad (4b)$$

the ratios of the radiative rates, $k_r(T_2)/k_r(T_1)$ and $k_r(S_1)/k_r(T_1)$, are obtained to be 3.0 and 233.5, respectively. Applying the value for τ^0 of $T_1(5 \times 10^{-3}$ s), the intrinsic lifetimes for T_2 and S_1 are obtained to be, respectively, 1.7×10^{-3} and 2.1×10^{-5} s for Q[1,0] vapor.[6]

As was mentioned, Q[0,0] in a neon host shows the $^3A_u(T_2)$ and $^3B_{1g}(T_1)$ phosphorescence at temperatures as low as 4.5 K.[54] Occurrence of the dual emission at such a low temperature is not surprising, since according to eq 4a the ratio $\Phi_P(T_2)/\Phi_P(T_1)$ is estimated to be 0.3 at 4.5 K for $\Delta E(T_2-T_1) = 11$ cm^{-1}, assuming $k_r(T_2)/k_r(T_1) = \sim 10$. The emission from the upper electronic states, due to the existence of two closely located states, have been observed not only with the direct electronic excitation, but with the infrared multiphoton excitation. Borisevich et al. have investigated the delayed fluorescence of Q[1,1] vapor induced by infrared multiphoton excitation.[131,133] The time evolution and pressure dependence of the observed delayed emission have been found to be similar to those excited electronically.

B. Photophysics in the Vapor Phase at Low Pressure

At low pressure where the molecules are almost free from collisions during the lifetime of the excited states, they exhibit intrinsic photophysical properties which are often different from those observed in the condensed phases or in the vapor phase at high total pressure. The nonfluorescent nature of the molecules containing C=O groups including quinones is usually attributed to the fast intersystem crossing from a $^1(n,\pi^*)$ to a $^3(\pi,\pi^*)$ state which is located higher in

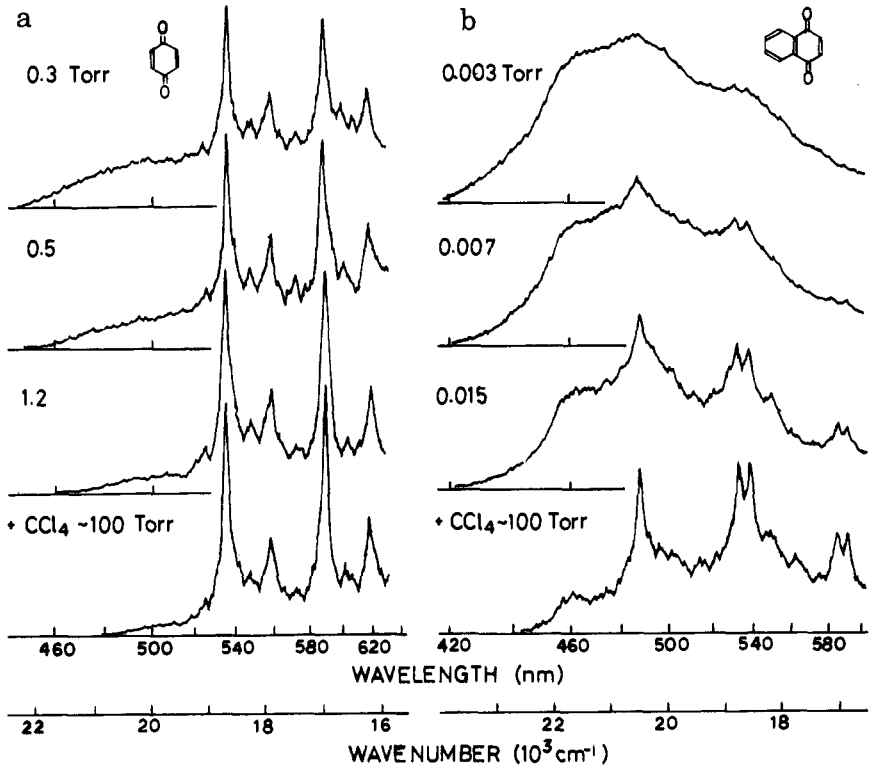

Figure 11. Emission spectra of Q[0,0] and Q[1,0] static vapors at different pressures.

energy than the lowest $^3(n,\pi^*)$ state.[179] However, when the molecule is free from collisions during the lifetime of the excited triplet state, it may return isoenergetically to the $S_1(n,\pi^*)$ state and may emit the fluorescence from S_1. Such a condition is normally achieved at pressures of 10^{-2}~10^{-3} Torr, where the intermolecular–collision interval is 10~100 μs. In fact, the emission which is regarded as originating from the singlet–triplet mixed state has been observed for Q[0,0][7,9] and Q[1,0] static vapors,[8] and possibly also for Q[1,1] vapor at low pressure.[15,132] The spectral shape of the emission from the mixed state is considered to be essentially the same as that of the $S_1(n,\pi^*)$ fluorescence, but the lifetime is significantly lengthened due to the dilution of $^1(n,\pi^*)$ presumably by $^3(\pi,\pi^*)$.[179]

Figure 11, parts a and b, respectively, show the emission spectra of Q[0,0] and Q[1,0] vapors at different pressures. As the pressure is reduced, the relative intensity of the $S_1(n,\pi^*)$ fluorescence increases and the emission spectra tend to be broad and intensified on the blue side.[8,9] In the case of the excitation into the $S_2(\pi,\pi^*)$ state, the fluorescence quantum yield (Φ_F) gradually increases as the pressure is reduced, whereas the phosphorescence quantum yield (Φ_P) decreases to approach zero for Q[0,0] and Q[1,0] static vapors (Figure 12).[8,9] Such an observation has been confirmed also by decay measurements as exemplified in Figure 13. At high total pressure, the fluorescence of Q[1,0] and Q[0,0] exhibits a single exponential decay with the lifetime being identical with the phosphorescence lifetime, but as the pressure is reduced the decay curve becomes a double exponential, with the lifetime of the fast decay component being pressure dependent and that of the slow one being identical with the phosphorescence lifetime.[7,8] Similar emission properties have been observed also for Q[1,1] static vapor, for which the relative intensity of the fluorescence to phosphorescence varies depending on the pressure and excitation energy.[15,131-134] These observations suggest that the fluorescence of Q[1,1] is originating at least in part from the singlet–triplet mixed state at reduced pressure.

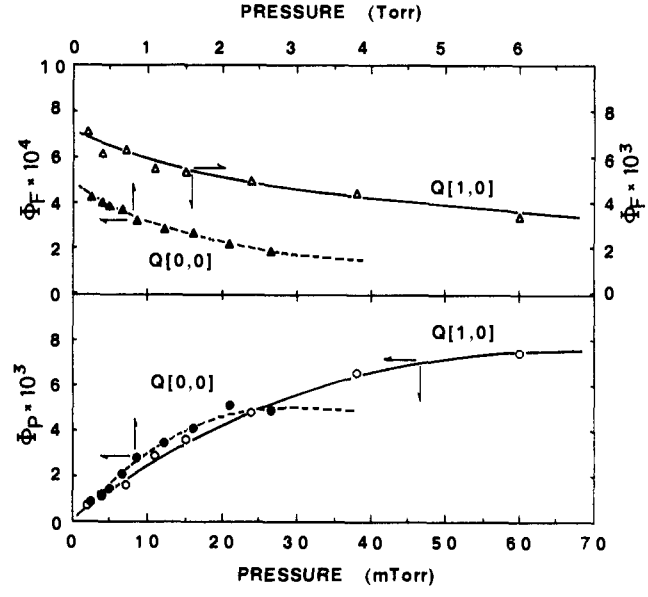

Figure 12. Pressure dependence of Φ_F and Φ_P for Q[0,0] and Q[1,0] vapors. The quantum yields are obtained by excitation into the $S_2(\pi,\pi^*)$ state.

On the basis of the pressure dependence of Φ_F and Φ_P as well as the emission lifetimes, the occurrence of the fluorescence from the mixed state has been interpreted kinetically in terms of a mechanism involving reversible intersystem crossing between the $S_1(n,\pi^*)$ and a triplet state T (Figure 14a), for which

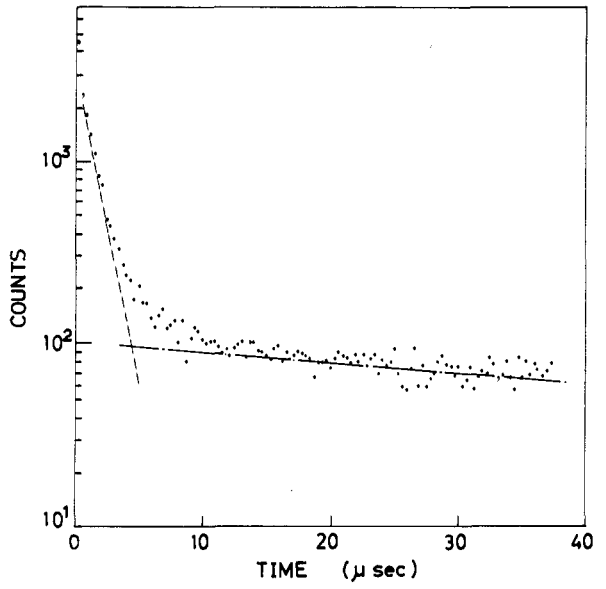

Figure 13. A typical double exponential decay curve of Q[1,0] static vapor at low pressure.

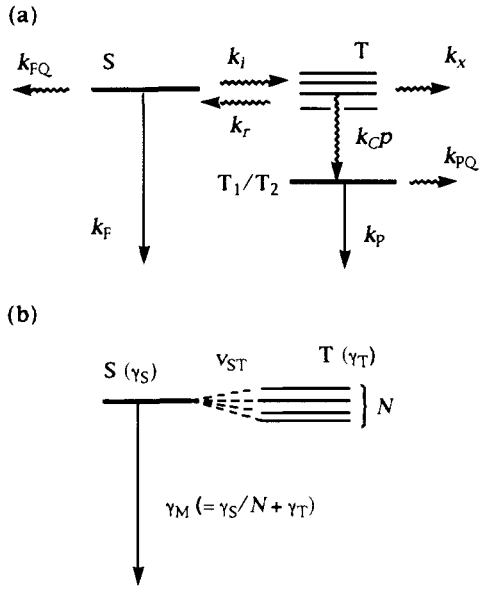

Figure 14. A scheme showing the electronic relaxation processes: (a) a kinetic scheme and (b) a quantum mechanical scheme.

Φ_F and Φ_P are given in the forms (Appendix B)

$$\Phi_F = k_F(k_x + k_Q p + k_r)/K \tag{5a}$$

$$\Phi_P = k_i k_Q p[k_P/(k_P + k_{PQ})]/K \tag{5b}$$

where $K = (k_F + k_{FQ})(k_x + k_Q p + k_r) + k_i(k_x + k_Q p)$ with $k_Q p$ denoting the effective rate constant at a particular pressure, p, for the collisional deactivation from higher vibrational levels of a triplet state to lower vibrational levels of the phosphorescent triplet state (T_1 and/or T_2). Hence, Φ_F normally increases with decreasing pressure, whereas Φ_P decreases to approach zero, as are indicated in Figure 12. It is also recognized from the kinetic scheme that the fluorescence at low pressure consists of fast and slow decay components: The fast one corresponds to the fluorescence directly emitted from the $S_1(n,\pi^*)$ state, while the slow one corresponds to the fluorescence which is emitted after the molecules return to the S_1 state from a triplet. If the quantum yields of the fast and slow components are denoted by Φ_F^{fast} and Φ_F^{slow}, respectively, then we obtain[8,9]

$$\Phi_F = \Phi_F^{fast} + \Phi_F^{slow} \tag{6}$$

where $\Phi_F^{fast} = k_F/X$ and $\Phi_F^{slow} = k_F k_i k_r/[(k_x + k_Q p)X^2 + k_r(k_F + k_{FQ})X]$ with $X = k_F + k_{FQ} + k_i$. By analyzing the pressure dependence of the emission quantum yields and lifetimes, the fluorescence at low pressure has been shown to consist mostly of the slow decay component (Φ_F^{slow}) for Q[0,0] and Q[1,0] static vapors.[8,9] An almost equivalent treatment can be applied for the description of the decay process of the singlet–triplet mixed state, using energy widths of the pure singlet (γ_S) and triplet states (γ_T) (Figure 14b).[10,11] Assuming the strong coupling betwen the singlet and triplet states, the width (or the decay rate) of the mixed state γ_M may be expressed as

$$\gamma_M = \gamma_S/N + \gamma_T \tag{7}$$

where N is the number of the triplet levels interacting with a singlet level.

Another notable photophysical behavior of para quinone static vapors at low pressure is that Φ_P shows an abrupt steplike decrease when the excitation energy is raised above the onset of the $S_0 \rightarrow S_2(\pi,\pi^*)$ excitation, although it is fairly constant over a whole range of the $S_0 \rightarrow S_1(n,\pi^*)$ excitation. This behavior has been observed clearly for Q[0,0] and Q[1,0] vapors.[8,9] A similar excitation energy dependence of Φ_P has been observed also for Q[1,1] vapor at the $S_3(\pi,\pi^*)$ threshold[94,96,98] as well as for other aromatic carbonyl compound vapors at the S_2 and S_3 thresholds.[181] Such an excitation energy dependence of Φ_P has been interpreted in terms of slow vibrational energy redistribution both in the triplet and singlet manifolds, thereby the molecule seems to transmit memory of the vibronic levels initially populated by a photon.[8,9,181]

In contrast to the experiments in static vapor, those in a supersonic jet expansion provide information on the intrinsic photophysical nature of cooled and isolated molecules in which the Boltzmann distribution is almost excluded. Unfortunately, supersonic jet experiments have been carried out only for Q[0,0].[10,11,44,45] In a jet, Q[0,0] shows the fluorescence from $^1B_{1g}$ and the phosphorescence from ^3A_u upon excitations into the $^1B_{1g}$ and ^3A_u states, respectively, although in static vapor the excitation into $^1B_{1g}$ brings about the emission both from $^1B_{1g}$ and ^3A_u. Recent studies of the photophysics of cooled and isolated Q[0,0] have been focused on the role of molecular rotation on the singlet–triplet coupling.[11] Ter Horst and Kommanduer have carried out Stern–Volmer-type experiments in a jet, by varying He stagnation pressure and excitation distance from the nozzle, to obtain the collision free lifetimes of the cooled vapor.[10] The observed $^1B_{1g}$ fluorescence lifetime increases with rotational quantum number, but at 2000 cm^{-1} above the $^1B_{1g}$ origin the rotational effects are masked by the singlet–triplet radiationless decay. Ohta et al. have recently reported the fluorescence decay following excitation at the indi-

vidual rotational lines of the vibronic bands in the $^1B_{1g}$ state, together with the excitation spectra in a jet.[11] The observed decay is nearly single exponential, but in some case a quantum beat is superimposed on the exponential decay. The fluorescence quantum yield is found to depend strongly on the rotational quantum number of the total angular momentum in the excited vibronic levels in $^1B_{1g}$, while the singlet−triplet coupling is extremely weak at the $^1B_{1g}$ origin. Suzuka et al. have measured the phosphorescence emission from Q[0,0] with the excitation into the ^3A_u origin in a jet.[45] The observed phosphorescence spectral pattern is almost identical with that in the static vapor, presumably indicating inefficient internal conversion from $^3A_u(n,\pi^*)$ to $^3B_{1g}$ (n,π^*) or near degeneracy of the two triplet states.

Only little is known for the photophysics of the linear para acenequinones other than Q[0,0], Q[1,0], and Q[1,1], but the photophysical nature of Q[3,0], Q[3,2], and Q[3,3] is expected to be similar to that of polyacenes.

VII. Summary

Considerable progress has been made during the past two decades on the spectroscopy and photophysics of linear para acenequinones. This has included a rigorous demonstration of the nature of the low-lying excited states and the photophysics of these species, occurrence of the dual or T_2 phosphorescence and the emission from the singlet−triplet mixed state, relationship between the state ordering and emission properties, location and symmetry nature of the excited states, and spin orbit and/or vibronic interaction mechanisms. The phosphorescence intensities of the linear para acenequinones having the $^3(n,\pi^*)$ state as the lowest triplet, are likely to be obtained primarily through the mechanisms involving a very small energy denominator between ^3A_u (n,π^*) and $^3B_{1g}(n,\pi^*)$ in the case of Q[0,0] and Q[1,1],[14,121] and that between $^3A_2(n,\pi^*)$ and $^3B_1(n,\pi^*)$ in the case of Q[1,0] (Appendix A).[6]

Para quinones of linear acenes form a unique group of organic molecules for which not only classical models have been applied to elucidate the excited-state dynamical behaviors, but also a number of modern techniques such as a thermal-lens method and supersonic jet expansions combined with two photon spectroscopy or with the sensitized excitation spectroscopy utilizing a triplet−triplet energy transfer, should be applied to get more detailed information on their photophysical properties as well as on the excited-state levels. With regard to the state levels, there still remain a number of significant challenges such as unambiguous identification of the two $^1(n,\pi^*)$ states of Q[1,0], determination of the $^3B_{1g}$ state of Q[0,0] vapor and that of the ^1A_u state of Q[1,1]. Photophysics of various derivatives of para quinones is also of interest. Since the introduction of substituents destroys the high symmetry of the parent molecules, it could influence the nature of the electronic states and photophysical properties. A group of these molecules, as well as the parent para quinones, can also be model systems for the tests of a number of modern nonradiative transition theories. Further efforts in these areas should provide a better understanding of the relationship between the photophysical properties and electronic structure of organic molecules which are not restricted to the present systems.

Appendix A

The singlet → triplet transition obtains its intensity directly by two possible mechanisms: (1) spin−orbit interaction between the excited triplet and an allowed singlet state and (2) spin−orbit interaction between the ground state and an excited triplet state. Thus, the oscillator strength for the $S_0 \rightarrow T_k$ transition, $f(S_0 - T_k)$, is expressed by

$$f(S_0-T_k) = f(S_i-S_0)[\Delta E(T_k-S_0)/\Delta E(S_i-S_0)] \times [\langle S_i|H_{so}|T_k\rangle/\Delta E(S_i-T_k)]^2 + f(T_j-T_k)[\Delta E(T_k-S_0)/\Delta E(T_k-T_j)] \times [\langle T_j|H_{so}|S_0\rangle/\Delta E(T_j-S_0)]^2 + \ldots \quad (A1)$$

where $\Delta E(i-j)$ is the energy difference between the states i and j, and H_{so} is a spin−orbit interaction operator. With D_{2h} quinones, the lower lying $^3(n,\pi^*)$ state is either ^3A_u or $^3B_{1g}$. In mechanism 1 (the first term in eq A1), only the two matrix elements, $\langle^1B_{1u}|H_{so}(b_{1g})|^3A_u\rangle$ and $\langle^1A_g|H_{so}(b_{1g})|^3B_{1g}\rangle$, must be important, since all the other possible combinations of S_i, T_k, and H_{so} eliminate the matrix element. Here, only the $R_z(b_{1g})$ component of H_{so} is considered to be effective in intensity borrowing: an $R_z(b_{1g})$ operation on the $n(2p_y)$ orbital causes it to overlap with the $\pi(2p_x)$ orbital, whereas $R_y(b_{2g})$ and $R_x(b_{3g})$ operations on the $n(2p_y)$ orbitals cause no overlap with the $\pi(2p_x)$ orbital. The transition $^1A_g(S_0) \rightarrow {}^1B_{1u}$ is allowed, while $^1A_g(S_0) \rightarrow {}^1A_g$ is forbidden $[(x,y,z) = (b_{3u},b_{2u},b_{1u})]$. Hence, the $S_0 \rightarrow T_k$ transition can obtain its intensity only when T_k is ^3A_u. In mechanism 2 also, with the same reasons mentioned above, only the matrix element $\langle^3B_{1g}|H_{so}(b_{1g})|^1A_g\rangle$ is important. That is, the state T_j in the second term of eq A1 is $^3B_{1g}$. Hence the $S_0 \rightarrow T_k$ transition can obtain its intensity only when T_k is ^3A_u ($\langle A_u|z|^3B_{1g}\rangle \neq 0$). In both mechanisms, the $^1A_g \rightarrow {}^3A_u$ transition is expected to be stronger than the $^1A_g \rightarrow {}^3B_{1g}$ transition.[14]

Direct spin−orbit interaction is not responsible for mixing the $^3B_{1g}$ state with allowed singlet states for D_{2h} quinones. In this case, one has to consider vibronic spin−orbit interaction for the mixing. On the basis of the Herzberg−Teller intensity borrowing mechanism, an equation formally similar to A1, but much more complicated one, can be derived. This equation involves the matrix elements for the first-, $\langle^3B_{1g}|(\partial H_{so}/\partial Q_\nu)_{Q\nu=0}|S_i\rangle$, and second-order vibronic spin−orbit interaction, $\langle^3B_{1g}|(\partial H_0/\partial Q_\nu)_{Q\nu=0}|T_k\rangle\langle T_k|H_{so}|S_i\rangle$ and $\langle^3B_{1g}|H_{so}|S_j\rangle\langle S_j|(\partial H_0/\partial Q_\nu)_{Q\nu=0}|S_i\rangle$, with Q_ν denoting the normal coordinate for the vibration ν and H_0 the Hamiltonian of the unperturbed system ($H = H_0 + H_{so} + \sum_\nu(\partial H_0/\partial Q_\nu)_{Q\nu=0}Q_\nu + \sum_\nu(\partial H_{so}/\partial Q_\nu)_{Q\nu=0}Q_\nu + \ldots$). Although there are a number of possible combinations for $[H_{so},Q_\nu,S_i]$, $[Q_\nu,T_k,H_{so},S_i]$, and $[H_{so},S_j,Q_\nu,S_i]$ that make the above matrix elements nonzero, it has been experimentally proven for Q[1,1] (and probably also for Q[0,0][38]) that the intensity borrowing is effective only when S_i is $^1B_{1u}(\pi,\pi^*)$ ($[H_{so}(b_{3g},b_{2g},b_{1g})$, $Q_\nu(b_{3u},b_{2u},b_{1u}),S_i(^1B_{1u})]$, $[Q_\nu(b_{3u},b_{2u},b_{1u}),T_k(^3B_{2u},^3B_{3u},$ $^3A_u),H_{so}(b_{3g},b_{2g},b_{1g}),S_i(^1B_{1u})]$ and $[H_{so}(b_{3g},b_{2g},b_{1g}),S_j$

$(^1B_{2g},^1B_{3g},^1A_g),Q_\nu(b_{3u},b_{2u},b_{1u}),S_i(^1B_{1u})])$.[119,121] Of course, the present treatment also accounts for the weakness of the transition between nonvibronic levels of the $^3B_{1g}$ and the ground state ^1A_g, i.e., the origin band.

Appendix B

According the kinetic scheme in Figure 13, we have the following set of differential equations:

$$(d/dt)\begin{pmatrix}[S]\\[T]\\[G]\end{pmatrix} = \begin{pmatrix}-(k_F+k_{FQ}+k_i) & k_r & k_0\\ k_i & -(k_q p+k_x+k_r) & 0\\ \cdots & \cdots & -k_0\end{pmatrix}\begin{pmatrix}[S]\\[T]\\[G]\end{pmatrix} \quad (B1)$$

where [S], [T], and [G] represent, respectively, the populations of the excited singlet, excited triplet, and ground states, and k_0 is the excitation rate constant of the ground state. In the case of steady-state excitation, the conditions, $(d/dt)[S] = (d/dt)[T] = 0$, hold. Hence, we obtain the relations among [S], [T], and [G] (for example, $[T] = [k_i/(k_F + k_{FQ} + k_r)][S]$). When these are substituted in the definition of the quantum yields, $\Phi_F = k_F[S]/k_0[G]$ and $\Phi_P = [k_P/(k_P + k_{PQ})] \times \Phi_T$ with $\Phi_T = k_q p\,[T]/k_0[G]$, we have eqs 5a and 5b in the text.

Acknowledgments. This work was supported in part by the Research Fund (1993 and 1994) of Kanto Junior College.

References

(1) Itoh, T.; Katsuolis, D. E.; Mita, I. *J. Mater. Chem.* **1993**, *3*, 1303.
(2) Miki, S.; Yoshida, Z. *Tetrahedron* **1992**, *48*, 1567.
(3) Morton, R. A. *Biochemistry of Quinones*; Academic Press: New York, 1965.
(4) (a) Baber, J. L.; Chan, I. Y. *J. Chem. Phys.* **1992**, *96*, 5591. (b) Becker, R. S.; Natarajan, L. V. *J. Phys. Chem.* **1993**, *97*, 344.
(5) Itoh, T.; Baba, H. *Bull. Chem. Soc. Jpn.* **1979**, *52*, 3213.
(6) (a) Itoh, T. *J. Chem. Phys.* **1987**, *87*, 4361. (b) Itoh, T. *J. Chem. Phys.* **1988**, *88*, 7257.
(7) Brus, L. E.; McDonald, J. R. *J. Chem. Phys.* **1973**, *58*, 4223.
(8) Itoh, T.; Baba, H. *Chem. Phys.* **1980**, *51*, 179.
(9) Itoh, T. *Mol. Phys.* **1985**, *55*, 799.
(10) Ter Horst, G.; Kommandeur, J. *J. Chem. Phys.* **1982**, *76*, 137.
(11) Ohta, N.; Yamazaki, I.; Sanekata, M.; Suzuka, I.; Sekiguchi, O. *J. Phys. Chem.* **1993**, *97*, 7857.
(12) Nepras, M.; Titz, M. *Int. J. Quantum Chem.* **1979**, *16*, 543.
(13) Nepras, M.; Fabian, J.; Titz, M. *Collect. Czech. Chem. Commun.* **1981**, *46*, 20.
(14) Hollas, J. M.; Goodman, L. *J. Chem. Phys.*, **1965**, *43*, 760.
(15) Itoh, T. unpublished data.
(16) Asundi, R. K.; Singh, R. S. *Nature* **1955**, *176*, 1223.
(17) Anno, T.; Sado, A. *J. Chem. Phys.* **1960**, *32*, 1602.
(18) Hollas, J. M. *Spectrochim. Acta* **1964**, *20*, 1563.
(19) Christoffersen, J.; Hollas, J. M. *Mol. Phys.* **1969**, *17*, 655.
(20) Sado, A. *Bull. Chem. Soc. Jpn.* **1962**, *35*, 1520.
(21) Eberhardt, W. H.; Renner, H. *J. Mol. Spectrosc.* **1961**, *6*, 483.
(22) (a) Trommsdorff, H. P. *J. Chem. Phys.* **1972**, *56*, 5358. (b) Trommsdorff, H. P. *Chem. Phys. Lett.* **1971**, *10*, 176.
(23) Trommsdorff, H. P.; Kahane-Paillous, J. *Spectrochim. Acta* **1967**, *23A*, 1661.
(24) Koyanagi, M. *J. Mol. Spectrosc.* **1968**, *25*, 273.
(25) McConnell, H. *J. Chem. Phys.* **1952**, *20*, 700.
(26) Braude, E. A. *J. Chem. Soc.* **1945**, 490.
(27) (a) Nagakura, S.; Kuboyama, A. *J. Am. Chem. Soc.* **1954**, *76*, 1003. (b) Nagakura, S.; Kuboyama, A. *J. Chem. Soc. Jpn.* **1953**, *74*, 499.
(28) Novak, A.; Titz, M.; Nepras, M. *Collect. Czech. Chem. Commun.* **1974**, *39*, 1532.
(29) Flaig, W.; Ploetz, Th.; Kullmer, A. *Z. Naturforsch.* **1955**, *10B*, 668.
(30) Kuboyama, A. *Bull. Chem. Soc. Jpn.* **1962**, *35*, 295.
(31) Baba, H. *J. Chem. Soc. Jpn.* **1951**, *72*, 341.
(32) Kanda, Y.; Kaseda, H.; Matsumura, T. *Spectrochim. Acta* **1964**, *20*, 1387.
(33) Herre, W.; Weis, P. *Chem. Phys. Lett.* **1970**, *7*, 276.
(34) (a) Sidman, J. W. *J. Am. Chem. Soc.* **1956**, *78*, 2363. (b) Sidman, J. W. *J. Chem. Phys.* **1957**, *27*, 820.
(35) Brand, J. C. D.; Goodwin, T. H. *Trans. Faraday Soc.* **1957**, *53*, 295.
(36) Trommsdorff, H. P. *Chem. Phys. Lett.* **1967**, *1*, 214.
(37) Hochstrasser, R. M.; Johnson, L. W.; Trommsdorff, H. P. *Chem. Phys. Lett.* **1973**, *21*, 251.
(38) Veenvliet, H.; Wiersma, D. A. *Chem. Phys.* **1975**, *8*, 432.
(39) Dunn, T. M.; Francis, A. H. *J. Mol. Spectrosc.* **1974**, *50*, 14.
(40) Kuboyama, A.; Matsuzaki, S.; Takagi, H.; Arano, H. *Bull. Chem. Soc. Jpn.* **1974**, *47*, 1604.
(41) Brint, P.; Connerade, J.-P.; Tsekeris, P.; Bolovinos, A.; Baig, A. *J. Chem. Soc., Faraday Trans. 2* **1986**, *82*, 367.
(42) Brint, P.; Tsekeris, P.; Bolovinos, A.; Kosmidis, C. *J. Chem. Soc., Faraday Trans. 2* **1989**, *85*, 177.
(43) Miyagi, Y.; Koyanagi, M.; Kanda, Y. *Bull. Chem. Soc. Jpn.* **1980**, *53*, 2502.
(44) Ter Horst, G.; Kommandeur, J. *Chem. Phys.* **1979**, *44*, 287.
(45) Suzuka, I.; Toda, H.; Nakajyo, T. *Proc. Symp. Mol. Struc. Jpn.* **1988**, 792.
(46) Koyanagi, M.; Miyagi, Y.; Kanda, Y. *J. Lumin.* **1976**, *12/13*, 345. (b) *Proc. Symp. Mol. Struc. Jpn.* **1976**, 230.
(47) Koyanagi, M.; Kogo, Y.; Kanda, Y. *J. Mol. Spectrosc.* **1970**, *34*, 450.
(48) Veenvliet, H.; Wiersma, D. A. *J. Chem. Phys.* **1974**, *60*, 704.
(49) Hunter, S. J.; Parker, H.; Francis, A. H. *J. Chem. Phys.* **1974**, *61*, 1390.
(50) Koyanagi, M.; Mitsuyasu, K.; Miyagi, Y. *J. Phys. Chem.* **1992**, *96*, 1578.
(51) Attia, A. I.; Loo, B. H.; Francis, A. H. *Chem. Phys. Lett.* **1973**, *22*, 537.
(52) Briegleb, G.; Herre, W.; Wolf, D. *Spectrochim. Acta* **1969**, *25A*, 39.
(53) Sebti, M.; Dupuy, F.; Nouchi, G.; Rousset, Y. *C. R. Acad. Sci.* **1970**, *270*, B1477.
(54) Goodman, J.; Brus, L. E. *J. Chem. Phys.* **1978**, *69*, 1604.
(55) Itoh, T. *Spectrochim. Acta* **1984**, *40A*, 387.
(56) Longin, P. *C. R. Acad.* **1970**, *271*, B292.
(57) (a) Jayswal, M. G.; Singh, R. S. *Spectrochim. Acta* **1965**, *21*, 1597. (b) Jayswal, M. G.; Singh, R. S. *J. Mol. Spectrosc.* **1965**, *17*, 6.
(58) Koyanagi, M.; Kogo Y.; Kanda, Y. *Mol. Phys.* **1971**, *20*, 747.
(59) Pandey, V. N.; Thakur, S. N. *Proc. Ind. Acad. Sci. (Chem. Sci.)* **1983**, *92*, 127.
(60) Veenvliet, H.; Wiersma, D. A. *Chem. Phys.* **1973**, *2*, 69.
(61) Veenvliet, H.; Wiersma, D. A. *Chem. Phys. Lett.* **1973**, *22*, 87.
(62) Sheng, S. J.; El-Sayed, M. A. *Chem. Phys. Lett.* **1975**, *34*, 216.
(63) Singh, S. N.; Singh, R. S. *Ind. J. Pure Appl. Phys.* **1968**, *6*, 187.
(64) Singh, S. N. *Ind. J. Pure Appl. Phys.* **1973**, *11*, 303.
(65) Daglish, C. *J. Am. Chem. Soc.* **1950**, *72*, 4859.
(66) Hartmann, H.; Lorenz, E. *Z. Naturforsch.* **1952**, *7A*, 360.
(67) Kuboyama, A. *Bull. Chem. Soc. Jpn.* **1958**, *31*, 752.
(68) Berg, H.; Kramarczyk, K. *Ber. Bunsen-Ges. Phys. Chem.* **1964**, *68*, 296.
(69) Shcheglova, N. A.; Shigorin, D. N. *Zh. Fiz. Khim.* **1964**, *38*, 1261.
(70) Dupuy, F.; Leibovici, C.; Sebti, M. *C. R. Acad. Sci.* **1966**, *263*, B1321.
(71) Zander, M. *Naturwissenschaften* **1966**, *53*, 404.
(72) Zander, M. *Ber. Bunsen-Ges. Phys. Chem.* **1967**, *71*, 424.
(73) Singh, I.; Ogata, R. T.; Moore, R. E.; Chang, C. W. J.; Scheuer, P. J. *Tetrahedron* **1968**, *24*, 6053.
(74) Kuboyama, A.; Yamazaki, R.; Yabe, S.; Uehara, Y. *Bull. Chem. Soc. Jpn.* **1969**, *42*, 10.
(75) Sidman, J. W. *J. Am. Chem. Soc.* **1956**, *78*, 4567.
(76) Galaup, J. P.; Megel, J.; Trommsdorff, H. P. *J. Chem. Phys.* **1978**, *69*, 1030.
(77) Fukuda, M.; Tajiri, A.; Oda, M.; Hatano, M. *Bull. Chem. Soc. Jpn.* **1983**, *56*, 592.
(78) Gottarelli, G.; Spada, G. P. *J. Chem. Soc., Parkin Trans. 2* **1984**, 1501.
(79) Titz, M.; Nepras, M. *Collect. Czech. Chem. Commun.* **1972**, *37*, 2674.
(80) Kuboyama, A.; Kozima, Y.; Maeda, J. *Bull. Chem. Soc. Jpn.* **1982**, *55*, 3635.
(81) Singh, S. N.; Singh, R. S. *Ind. J. Pure Appl. Phys.* **1967**, *5*, 394.
(82) Singh, R. S. *Ind. J. Pure Appl. Phys.* **1968**, *6*, 91.
(83) Kuboyama, A.; Yabe, S. *Bull. Chem. Soc. Jpn.* **1967**, *40*, 2475.
(84) Vo-Dinh, T.; Wild, U. P. *Spectrochim. Acta* **1984**, *40A*, 411.
(85) Nepras, M.; Novak, A. *Collect. Czech. Chem. Commun.* **1977**, *42*, 2343.
(86) Shigorin, V. D.; Shipulo, G. P. *Zh. Prikl. Spektrosk.* **1970**, *12*, 331.
(87) Yamanashi, B. S.; Hercules, D. M. *Appl. Spectrosc.* **1971**, *25*, 457.
(88) Shigorin, D. N.; Tushishvili, L. Sh.; Shcheglova, N. A.; Dokunikhin, N. S. *Zh. Fiz. Khim.* **1971**, *45*, 511.
(89) Vo-Dinh, T.; Paetzold, R.; Wild, U. P. *Z. Phys. Chem. (Leipzig)* **1972**, 251, 395.

(90) Strokach, N. S.; Brivina, L. P.; Shigorin, D. N.; Gorelik, M. V. *Zh. Fiz. Khim.* **1981**, *55*, 1211.
(91) Kuboyama, A. *Bull. Chem. Soc. Jpn.* **1978**, *51*, 2771.
(92) Diaz, A. N. *J. Photochem. Photobiol. A* **1990**, *53*, 141.
(93) Tolkachev, V. A.; Borisevich, N. A. *Opt. Spektrosk.* **1965**, *18*, 388.
(94) Borisevich, N. A.; Tolkachev, V. A. *Opt. Spektrosk.* **1966**, *21*, 36.
(95) Singh, S. N.; Singh, R. S. *Ind. J. Pure Appl. Phys.* **1967**, *5*, 245.
(96) Borisevich, N. A.; Kotov, A. A.; Tolstorozhev, G. B. *Izv. Akad. Nauk SSSR, Ser. Fiz.* **1972**, *36*, 935.
(97) Borisevich, N. A.; Gruzinskii, V. V.; Kotov, A. A. *Izv. Akad. Nauk SSSR, Ser. Fiz.* **1970**, *34*, 490.
(98) Borisevich, N. A.; Kotov, A. A. *Dokl. Akad. Nauk BSSR* **1970**, *14*, 798.
(99) Reta, M. R.; Cattana, R.; Anunziata, J. D.; Silber, J. J. *Spectrochim. Acta* **1993**, *49A*, 903.
(100) Yoshimoto, T. *J. Chem. Soc. Jpn.* **1963**, *84*, 733.
(101) Kuboyama, A. *Bull. Chem. Soc. Jpn.* **1979**, *52*, 329.
(102) Itoh, T. *Spectrochim. Acta* **1986**, *42A*, 1083.
(103) Matsuzaki, S.; Kuboyama, A. *Kagaku Gijyutu Kenkyusho Houkoku* **1986**, *81*, 123.
(104) (a) Myrvold, B. O.; Spanget-Larsen, J.; Thulstrup, E. W. *Chem. Phys.* **1986**, *104*, 305. (b) Popov, K. P. *Opt. Spektrosk.* **1958**, *4*, 404.
(105) Borisevich, N. A.; Gruzinskii, V. V. *Izv. Akad. Nauk SSSR, Ser. Fiz.* **1960**, *24*, 545.
(106) Kunavin, N. I.; Shvekhgeimer, G. A. *Zh. Prikl. Spektrosk.* **1990**, *53*, 502.
(107) Nakamoto, K. *J. Am. Chem. Soc.* **1952**, *74*, 392.
(108) Narisawa, T.; Sano, M.; Ihaya, Y. J.; *Chem. Lett.* **1975**, 1289.
(109) Drabe, K. E.; Veenvliet, H.; Wiersma, D. A. *Chem. Phys. Lett.* **1975**, *35*, 469.
(110) Galaup, J. P.; Megel, J.; Trommsdorff, H. P. *Chem. Phys. Lett.* **1976**, *41*, 397.
(111) Kanezaki, E.; Nishi, N.; Kinoshita, M. *Bull. Chem. Soc. Jpn.* **1979**, *52*, 2836.
(112) (a) Dearman, H. H.; Sundarachari, N.; Ulku, D. *J. Chem. Phys.* **1966**, *45*, 4363. (b) Drott, H. R.; Dearman, H. H. *J. Chem. Phys.* **1967**, *47*, 1896.
(113) Bial, M. S.; Rana, A. M.; Saleh, M.; Ashraf, C. M. *J. Mater. Sci.* **1993**, *28* 6159.
(114) Bolotnikova, T. N.; Naumova, T. M.; Savchenkov, V. I. *Opt. Spektrosk.* **1979**, *47*, 684.
(115) Bolotnikova, T. N.; Naumova, T. M.; Savchenkov, V. I.; Chigirev, A. R. *Zh. Prikl. Spektrosk.* **1980**, *32*, 860.
(116) Singh, S. N.; Singh, R. S. *Indian J. Pure Appl. Phys.* **1967**, *5*, 342.
(117) Smirnov, N. S.; Gastilovich, E. A.; Shigorin, D. N. *Opt. Spektrosk.* **1973**, *35*, 238.
(118) Khalil, O. S.; Goodman, L. *J. Phys. Chem.* **1976**, *80*, 2170.
(119) Strokach, N. S.; Shigorin, D. N. *Opt. Spektrosk.* **1977**, *43*, 64.
(120) Lehmann, K. K.; Smolarek, J.; Khalil, O. S.; Goodman, L. *J. Phys. Chem.* **1979**, *83*, 1200.
(121) Murao, T.; Azumi, T. *J. Chem. Phys.* **1979**, *70*, 4460.
(122) Avarmaa, R.; Suisalu, A. *Izv. Akad. Nauk. ESSR* **1975**, *24*, 444.
(123) Kuboyama, A. *Bull. Chem. Soc. Jpn.* **1970**, *43*, 3373.
(124) Strokach, N. S.; Shigorin, D. N. *Opt. Spektrosk.* **1977**, *43*, 687.
(125) Strokach, N. S.; Shigorin, D. N. *Opt. Spektrosk.* **1978**, *45*, 454.
(126) Lewis, G.; Kasha, M. *J. Am. Chem. Soc.* **1944**, *66*, 2100.
(127) Hamanoue, K.; Nakayama, T.; Kajiwara, Y.; Yamaguchi, T.; Teranishi, H. *J. Chem. Phys.* **1987**, *86*, 6654.
(128) (a) Shigorin, D. N.; Shcheglova, N. A.; Dokunikhin, N. S.; Puchkov, V. A. *Dokl. Akad. Nauk SSSR* **1960**, *132*, 1372. (b) Hamanoue, K.; Nakayama, T.; Yamaguchi, T.; Ushida, K. *J. Phys. Chem.* **1989**, *93*, 3814.
(129) Carlson, S. A.; Hercules, D. M. *J. Am. Chem. Soc.* **1971**, *93*, 5611.
(130) Rogozhin, K. L.; Rodionov A. N.; Shigorin, D. N. *Opt. Spektrosk.* **1982**, *52*, 925.
(131) Borisevich, N. A. *Acta Phys. Pol.* **1987**, *A71*, 683.
(132) Emel'yanov, A. P.; Povedajlo, V. A.; Tolkachev, V. A. *Dokl. Akad. Nauk SSSR* **1989**, *33*, 789.
(133) Borisevich, N. A.; Zalesskaya, G. A.; Urbanovich, A. E. *Spectrosc. Lett.* **1990**, *23*, 405.
(134) Shcheglova, N. A.; Lesnenko, L. G. *Opt. Spektrosk.* **1971**, *31*, 360.
(135) (a) Gas, B.; Stepan, V.; Titz, M.; Kratochvil, V.; Nepras, M. *Collect. Czech. Chem. Commun.* **1983**, *48*, 538. (b) Nepras, M.; Kratochvil, V.; Stepan, V.; Titz, M.; Gas, B. *Collect. Czech. Chem. Commun.* **1983**, *48*, 976.
(136) Kon, H. *Bull. Chem. Soc. Jpn.* **1955**, *28*, 275.
(137) Anno, T.; Sado, A.; Matsubara, I. *J. Chem. Phys.* **1957**, *26*, 967.
(138) Anno, T.; Matsubara, I.; Sado, A. *Bull. Chem. Soc. Jpn.* **1957**, *30*, 168.
(139) Leibovici, C.; Deschamps, J. *C. R. Acad. Sci.* **1965**, *261*, 5487.
(140) Leibovici, C.; Deschamps, J. *Theor. Chim. Acta* **1966**, *4*, 321.
(141) Nishimoto, K.; Forster, L. S. *Theor. Chim. Acta* **1966**, *4*, 155.
(142) Klessinger, M. *Theor. Chim. Acta* **1966**, *5*, 251.
(143) Plotnikov, V. G. *Opt. Spektrosk.* **1966**, *20*, 394.
(144) Leibovici, C.; Dupuy, F.; Deschamps, J. *C. R. Acad. Sci. Paris* **1967**, *264B*, 299.
(145) Flurry, R. L.; Stout, E. W.; Bell, J. J. *Theor. Chim. Acta* **1967**, *8*, 203.
(146) Adams, O. W.; Miller, R. L. *Theor. Chim. Acta* **1968**, *12*, 151.
(147) Edwards, T. G.; Grinter, R. *Mol. Phys.* **1968**, *15*, 357.
(148) Mishra, P. C.; Pandey, A. K. *Spectrosc. Lett.* **1975**, *8*, 953.
(149) Hoffmann, H.; Rasch, G. *Z. Phys. Chem. (Leipzig)* **1976**, *257*, 689.
(150) Fabian, J.; Mehlhorn, A. *Z. Chem.* **1978**, *18*, 338.
(151) Hug, W.; Kuhn, J.; Seibold, K. J.; Labhart, H.; Wagniere, G. *Helv. Chim. Acta* **1971**, *54*, 1451.
(152) Stevenson, P. E. *J. Phys. Chem.* **1972**, *76*, 2424.
(153) Masmanidis, C. A.; Jaffe, H. H.; Ellis R. L. *J. Phys. Chem.* **1975**, *79*, 2052.
(154) Merienne-Lafore, M. F.; Trommsdorff, H. P. *J. Chem. Phys.* **1976**, *64*, 3791.
(155) Cucchiara, G.; Dovesi, R.; Ricca, F.; Cerruti, L. *J. Mol. Struct.* **1978**, *43*, 61.
(156) Bigelow, R. W. *J. Chem. Phys.* **1978**, *68*, 5086.
(157) Jacques, P.; Faure, J.; Chalvet, O.; Jaffe, H. H. *J. Phys. Chem.* **1981**, *85*, 473.
(158) Sen, R.; Bhattacharyya, S. *Ind. J. Pure Appl. Phys.* **1986**, *24*, 348.
(159) Edwards, T. G.; Grinter, R. *Theor. Chim. Acta* **1968**, *12*, 387.
(160) Bunce, N. J.; Ridley, J. E.; Zerner, M. C. *Theor. Chim. Acta* **1977**, *45*, 283.
(161) Gleghorn, J. T.; McConkey, F. W. *J. Mol. Struc.* **1973**, *18*, 219.
(162) Bloor, J. E.; Paysen, R. A.; Sherrod, R. E. *Chem. Phys. Lett.* **1979**, *60*, 476.
(163) Asbrink, L.; Bieri, G.; Fridh, C.; Lindholm, E.; Chong, D. P. *Chem. Phys.* **1979**, *43*, 189.
(164) Hammond, H. A. *Theor. Chim. Acta* **1970**, *18*, 239.
(165) Hilal, R. *Int. J. Quantum Chem.* **1979**, *15*, 37.
(166) Wood, M. H. *Theor. Chim. Acta* **1975**, *36*, 345.
(167) Ha, T. K. *Mol. Phys.* **1983**, *49*, 1471.
(168) Martin, R. L. *J. Chem. Phys.* **1981**, *74*, 1852.
(169) Martin, R. L.; Wadt, W. R. *J. Phys. Chem.* **1982**, *86*, 2382.
(170) Ball, J. R.; Thomson, C. *Theor. Chim. Acta* **1988**, *74*, 195.
(171) Casado, J.; Peleterio, J.; Rios, M. A. *Chem. Phys. Lett.* **1979**, *62*, 349.
(172) Edwards, T. G. *Theor. Chim. Acta* **1973**, *30*, 267.
(173) Olbrich, G.; Polansky, O. E.; Zander, M. *Ber. Bunsen-Ges. Phys. Chem.* **1977**, *81*, 692.
(174) Kuboyama, A.; Wada, K. *Bull. Chem. Soc. Jpn.* **1966**, *39*, 1874.
(175) Pilipenko, A. T.; Savranskii, L. S. *Opt. Spektrosk.* **1970**, *28*, 808.
(176) Nepras, M.; Fabian, J.; Titz, M.; Gas, B. *Collect. Cezch. Chem. Commun.* **1982**, *47*, 2569.
(177) Petke, J. D.; Butler, P.; Maggiora, G. M. *Int. J. Quantum Chem.* **1985**, *27*, 71.
(178) Leibovici, C.; Deschamps, J. *C. R. Acad. Sci. Ser. C* **1967**, *264*, 70.
(179) (a) Lower, S. K.; El-Sayed, M. A. *Chem. Rev.* **1966**, *66*, 199. (b) El-Sayed, M. A. *J. Chem. Phys.* **1963**, *38*, 2834.
(180) Plotnikov, V. G. *Opt. Spektrosk.* **1967**, *23*, 39.
(181) (a) Itoh, T.; Takemura, T.; Baba, H. *Chem. Phys. Lett.* **1976**, *40*, 481. (b) Itoh, T.; Baba, H.; Takemura, T. *Bull. Chem. Soc. Jpn.* **1978**, *51*, 2841. (c)Itoh, T. *J. Phys. Chem.* **1985**, *89*, 3949. (d) Itoh, T. *Chem. Phys. Lett.* **1987**, *133*, 254. (e) Itoh, T. *J. Photochem. Photobiol. A* **1989**, *50*, 171. (f) Itoh, T. *Spectrochim. Acta A*, in press.

CR940054P